PAPER

CrossMark
click for updates

Design and synthesis of pyrazole/isoxazole linked arylcinnamides as tubulin polymerization inhibitors and potential antiproliferative agents†

Ahmed Kamal,*[a,b] Anver Basha Shaik,[a] Bala Bhaskara Rao,[c] Irfan Khan,[a] G. Bharath Kumar[a] and Nishant Jain[c]

As pyrazole and isoxazole based derivatives are well-known for displaying a considerable biological profile, an attempt has been made to unravel their cytotoxic potential. In this context, a number of pyrazole/isoxazole linked arylcinnamide conjugates (**15a–o** and **21a–n**) have been synthesized by employing a straight forward route. The basic structure comprised three ring scaffolds (A, B and C): methoxyphenyl rings as A and C rings and a five membered heterocyclic ring (pyrazole or isoxazole) as the B-ring. To achieve clear understanding, these derivatives are categorized as pyrazole-phenylcinnamides (**PP**) and isoxazole-phenylcinnamides (**IP**). These compounds have been evaluated for their ability to inhibit the growth of various human cancer cell lines such as HeLa, DU-145, A549 and MDA-MB231 and most of them exhibit considerable cytotoxic effects. Some of them like **15a**, **15b**, **15e**, **15i** and **15l** exhibit promising cytotoxicity in HeLa cells (IC$_{50}$ = 0.4, 1.8, 1.2, 2.7 and 1.7 μM). Amongst them **15a**, **15b** and **15e** were taken up for detailed biological studies, they were found to arrest the cells in the G2/M phase of the cell cycle. Moreover, they were investigated for their effect on the microtubular cytoskeletal system by using a tubulin polymerization assay, immunofluorescence and molecular docking studies; interestingly they demonstrate a significant inhibition of tubulin polymerization.

Introduction

Microtubules are important protein biopolymers formed through polymerization of α,β-tubulin heterodimers. The function of tubulin polymerization is reversible and the dynamic assembly and disassembly of microtubules occur in a number of cellular activities, including cell division, migration and morphological alteration.[1,2] In addition, microtubules are involved in a host of cell signaling pathways related to apoptosis. Consequently, microtubule network has become an important drug target in the design of newer antimitotic cytotoxic agents. Drugs that inhibit microtubule polymerization are effective in the treatment of lung, breast, ovarian, and other cancers. These drugs disrupt the dynamic equilibrium of

[a]*Medicinal Chemistry and Pharmacology, CSIR – Indian Institute of Chemical Technology, Hyderabad 500007, India. E-mail: ahmedkamal@iict.res.in*
[b]*Catalytic Chemistry Research Chair, Chemistry Department, College of Science, King Saud University, Riyadh 11451, Saudi Arabia*
[c]*Centre for Chemical Biology, CSIR – Indian Institute of Chemical Technology, Hyderabad 500007, India*
†Electronic supplementary information (ESI) available: ^{1}H NMR and ^{13}C NMR spectra of the conjugates and experimental procedures for biological activities. See DOI: 10.1039/c5ob01257k

tubulin polymerization, thereby inducing mitotic arrest. Moreover, various categories of drugs that are used for inhibiting microtubule dynamics, include taxanes, vinca alkaloids and colchicines.[3] Taxanes accelerate the polymerization of tubulin by stabilizing the assembled microtubules whereas the latter candidates depolymerise the tubulin by destabilising the microtubule.

Based on the literature it is well established that the microtubules possess three important ligand binding sites namely vinca domain, colchicine domain and taxan sites.[4–6] These sites specifically recognized in the α/β-tubulin heterodimers and the agents that interact with them are the foremost focus of the current researchers.[4–6] Some of the most important tubulin-binding agents that are employed as positive controls for the tubulin depolimerisation assay are colchicine (**1**), combretastatin A-4 (CA-4) (**2**) and nocodazole (**3**) (Fig. 1).[7–11] CA-4 is a natural *cis*-stilbene that has a strong inhibitory effect on tubulin polymerization by binding at the colchicine binding site.[12–14]

Pyrazole and isoxazole molecular scaffolds have gained much attention for research in medicinal chemistry and many investigations on their synthesis as well as biological activities have been reported.[15] Recently analogs of combretastatin A-4 (CA-4) and 3,4-diarylpyrazoles were concisely synthesized,
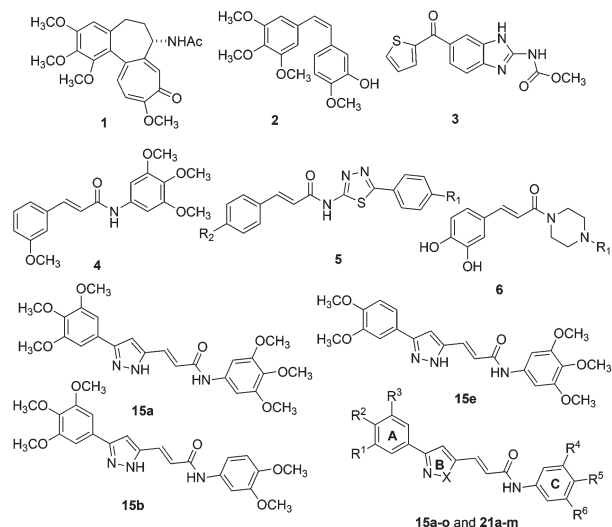
Fig. 1 Structures of some cytotoxic agents: colchicine (**1**), combretastatin-A4 (**2**), nocodazole (**3**), phenylcinnamides (**4**), thiadiazole ring based cinnamide (**5**), acrylylpiperazine (**6**), most active compounds (**15a**, **15b** and **15e**), pyrazole/isoxazole linked arylcinnamide conjugates (**15a–o** and **21a–m**).

among which, 3-methoxy-6-[4-(3,4,5-trimethoxyphenyl)-1*H*-pyrazol-3-yl]benzene-1,2-diol exhibits low nanomolar potency towards the cytotoxic and anti-tubulin activities.[16,17] Hergenrother and coworkers have synthesized some phenylcinnamides (**4**) that cause cytotoxicity in various human cancer cell lines apart from the accumulation of cells at the G2/M-phase of the cell cycle. Further investigations on cinnamide derivatives suggested that they exert their potential cytotoxic effects through the disruption of the microtubule network.[18a,b] Moreover, some 1,3,4-thiadiazole ring based cinnamide derivatives (**5**) showed a higher growth inhibition effect against MCF-7 and A549 cell lines apart from potent tubulin polymerization inhibitory activity.[19] In addition, a series of (*E*)-3-(3,4-dihydroxyphenyl)acrylylpiperazine conjugates (**6**) displayed potential cytotoxic activity in a panel of cancer cell lines that showed significant inhibition of tubulin polymerization.[20]

Based on the recent reports it is acknowledged that the derivatives of pyrazole, isoxazole and phenylcinnamides play a more significant role towards the development of potential cytotoxic agents.[21–23]

Previously we have reported that a series of pyrazole based conjugates have shown profound cytotoxic effects by arresting the cells in the G2/M phase.[24–26] In view of the attractive biological activities exhibited by them, considerable interest in the development of newer cytotoxic agents has been aroused. The present work illustrates the design and synthesis of some pyrazole/isoxazole linked arylcinnamide conjugates and evaluates their ability to inhibit the growth of a panel of four human cancer cell lines. The cellular effects shown by these compounds have been discussed in the following sections. All the desired compounds comprised three ring molecular scaffolds (A, B and C): different methoxy and fluro substituted

phenyl rings anchored on the A and C rings, while a five membered pyrazole or isoxazole as the B ring (Fig. 1).
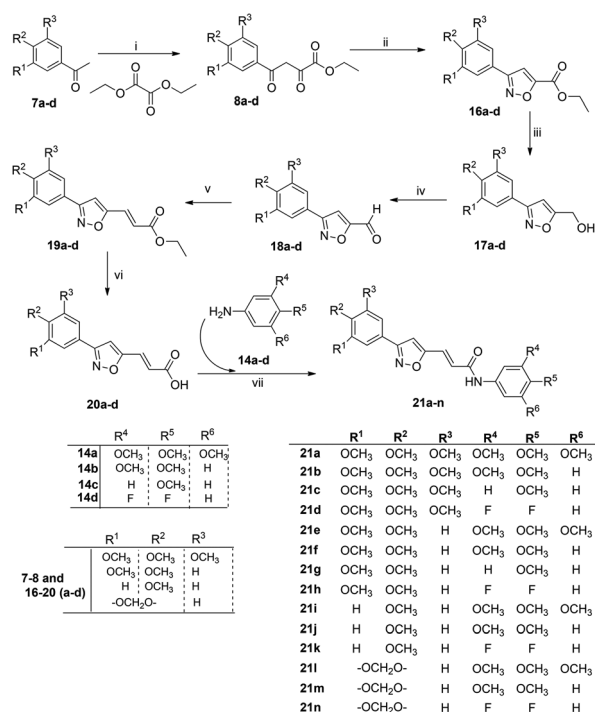
Results and discussion

Chemistry

The synthesis of pyrazole linked phenylcinnamide conjugates **15a–o** described in this work is outlined in Scheme 1. The synthesis was initiated with the sodium ethoxide-mediated condensation of different acetophenones **7a–d** with diethyl oxalate. The diketoesters **8a–d** thus obtained were converted to their corresponding pyrazole esters **9a–d** upon treatment with hydrazine in ethanol. In the next step, lithium aluminium hydride reduction of these esters afforded the corresponding primary alcohols **10a–d**. These were oxidized to the pyrazole carbaldehydes (**11a–d**) by using IBX in DMSO.[24] These pyrazole carbaldehydes upon reaction with (carbethoxymethylene)triphenylphosphine, $Ph_3PCHCO_2C_2H_5$ (C2-Wittig salt) in toluene afforded α,β-unsaturated esters **12a–d** that subsequently underwent a base hydrolysis to give α,β-unsaturated carboxylic acids **13a–d**.[26,27] Finally, these carboxylic acids conveniently coupled with substituted arylamines **14a–d** in the presence of EDC/Hobt produce the desired pyrazole linked phenylcinnamides (**PP**).[19] By employing the same methodology isoxazole linked
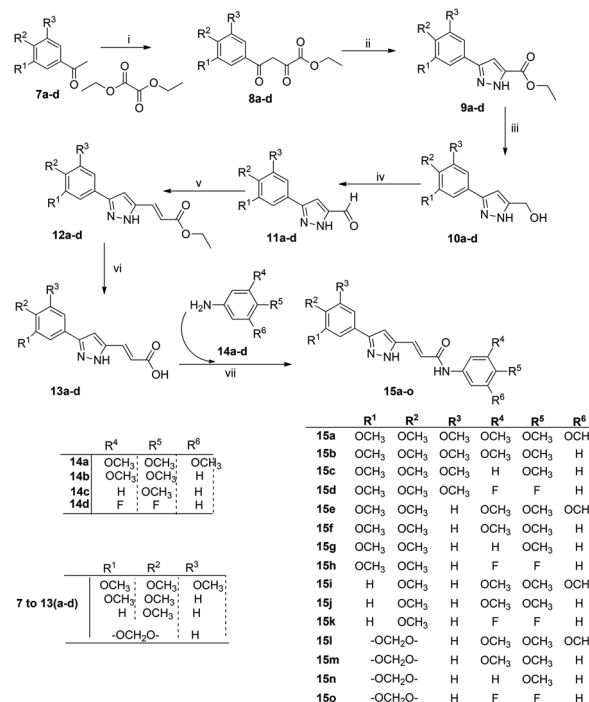
Scheme 1 Synthesis of pyrazole linked arylcinnamide conjugates. Reagents and conditions: (i) NaOEt, EtOH, 4 h, 0 °C–rt, (85–90%); (ii) NH_2–NH_2·2HCl, EtOH, 3–4 h, reflux, (70–80%); (iii) LiAlH₄, THF, 1–2 h, 0 °C–rt, (75–80%); (iv) IBX, dry DMSO, 1 h, rt (80–85%); (v) $Ph_3PCHCO_2C_2H_5$, toluene, 4 h, rt, (70–75%); (vi) LiOH·H₂O, THF : MeOH : H₂O (3 : 1 : 1), 3–4 h, rt; (80–85%) (vii) EDC/Hobt, dry CH_2Cl_2 + DMF, 8 h, 0 °C–rt (60–80%).

phenylcinnamide conjugates **21a–n** were synthesized starting from isoxazole esters (**16a–d**) as shown in Scheme 2. The latter esters were obtained when diketoesters **8a–d** were treated with hydroxylamine hydrochloride in refluxing ethanol.[25] Subsequently these esters underwent a sequential reduction and oxidation to afford isoxazole carbaldehydes **18a–d** that reacted with $Ph_3PCHCO_2C_2H_5$ (C2-Wittig reagent) in toluene to yield α,β-unsaturated esters **19a–d**. Selective oxidation of pyrazole or isoxazole alcohols is very critical as used IBX in DMSO. Due to miscibility of DMSO in ethyl acetate, crushed ice was added to the reaction mixture after extraction with ethyl acetate to obtain the DMSO free product. These unsaturated esters underwent a base hydrolysis to give the corresponding carboxylic acids **20a–d** that were coupled with different anilines to afford the desired isoxazole linked phenylcinnamides (**IP**). Some sort of difficulty was observed when the crude compounds of pyrazoles and isoxazole aryl cinnamides were washed with $NaHCO_3$, water and dil. HCl. From the starting point of synthesis we observed that all the reaction products of pyrazoles were more polar when compared to isoxazole reaction products. The pyrazole conjugates eluted very slowly from the column as they are highly polar when compared to isoxazole conjugates. All the synthesized compounds were characterized by standard spectroscopic analysis such as IR, ^{1}H NMR, ^{13}C NMR, and HRMS spectra.
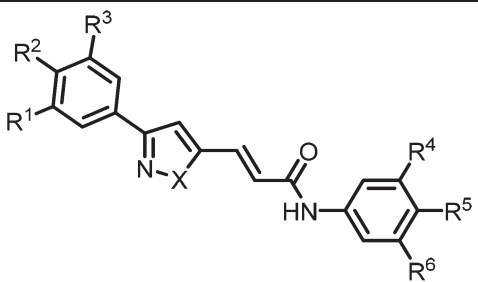

	R^4	R^5	R^6
14a	OCH_3	OCH_3	OCH_3
14b	OCH_3	OCH_3	H
14c	H	OCH_3	H
14d	F	F	H

	R^1	R^2	R^3
7-8 and 16-20 (a-d)	OCH_3	OCH_3	OCH_3
	OCH_3	OCH_3	H
	H	OCH_3	H
	-OCH_2O-		H

	R^1	R^2	R^3	R^4	R^5	R^6
21a	OCH_3	OCH_3	OCH_3	OCH_3	OCH_3	OCH_3
21b	OCH_3	OCH_3	OCH_3	OCH_3	OCH_3	H
21c	OCH_3	OCH_3	OCH_3	H	OCH_3	H
21d	OCH_3	OCH_3	OCH_3	F	F	H
21e	OCH_3	OCH_3	H	OCH_3	OCH_3	OCH_3
21f	OCH_3	OCH_3	H	OCH_3	OCH_3	H
21g	OCH_3	OCH_3	H	H	OCH_3	H
21h	OCH_3	OCH_3	H	F	F	H
21i	H	OCH_3	H	OCH_3	OCH_3	OCH_3
21j	H	OCH_3	H	OCH_3	OCH_3	H
21k	H	OCH_3	H	F	F	H
21l	-OCH_2O-		H	OCH_3	OCH_3	OCH_3
21m	-OCH_2O-		H	OCH_3	OCH_3	H
21n	-OCH_2O-		H	F	F	H

Scheme 2 Synthesis of isoxazole linked arylcinnamide conjugates. Reagents and conditions: (i) NaOEt, EtOH, 4 h, 0 °C−rt (85−90%); (ii) NH_2−OH·HCl, EtOH, 3 h, reflux, (75−80%); (iii) LiAlH₄, THF, 1−2 h, 0 °C−rt (70−80%); (iv) IBX, dry DMSO, 1 h, rt (80−85%); (v) $Ph_3PCHCO_2C_2H_5$, toluene, 4 h, rt (70−75%); (vi) LiOH·H_2O, THF : MeOH : H_2O (3 : 1 : 1) 3−4 h, rt (80−85%); (vii) EDC/Hobt, dry CH_2Cl_2 + DMF, 8 h, 0 °C−rt (65−78%).

Biology

Cytotoxic activity. To investigate the cytotoxic potential of these phenylcinnamides we evaluated the antiproliferative activity on different cancer cell lines like HeLa (cervical cancer), DU-145 (prostate cancer), A549 (lung adenocarcinoma) and MDA-MB231 (breast carcinoma). The results are summarized in Table 1 and nocodazole was employed as a standard. Both the types of compounds (**PP** and **IP**) bearing the cinnamoyl moiety exhibited significant antiproliferative activity. Some of the conjugates of **PP** possessing pyrazole as the B-ring displayed profound cytotoxicity that is comparable with the reference standard. Based on the obtained results most of the conjugates (**15a**, **15b**, **15e**, **15i** and **15l**) possessing pyrazole as the B-ring exhibited promising cytotoxicity in HeLa cells (IC_{50} range 0.4–2.7 μM) and the results were comparable with positive control, nocodazole. Whereas some of the conjugates **21a**, **21b** and **21e** that contain isoxazole as the B-ring also showed moderate cytotoxicity, however, reduced activity was observed when compared to pyrazole containing conjugates. All the compounds having electron donating methoxy/methylenedioxy groups on their A-ring and electron donating methoxy as well as electron withdrawing groups like fluoro on the C-ring have been examined. Among these compounds **15a**, **15e**, **15i** and **15l** bearing trimethoxy substituents on the C-ring have shown significant cytotoxicity with the highest inhibitory effect against HeLa cells, whereas **21a**, **21e**, **21i** and **21l** inhibit the growth of cells moderately. The lead compounds **15a** and **15e** with trimethoxy and dimethoxy groups on the A-ring and a similar substitution on the C-ring showed excellent potency in HeLa cells with IC_{50} values of 0.4 μM and 1.2 μM respectively. However, the presence of monomethoxy and 3,4-(methylenedioxy) groups on the A-ring diminished the cytotoxic effect (IC_{50} = 2.7 μM for **15i** and IC_{50} = 1.7 μM for **15l** in HeLa cells). In addition, the representative compounds inhibit the growth of MDA-MB231 cells significantly (IC_{50} = 1.0 μM, 1.6 μM, 3.8 μM and 2.3 μM). Further promising activity was also observed in dimethoxy substituted derivatives, C-ring like **15b** (1.8 μM), **15f** (5.5 μM), **15j** (13.5 μM) and **15m** (12.2 μM), whereas **21b**, **21f**, **21j** and **21m** showed moderate effects. However, monomethoxy substituted derivatives showed deleterious effects on cytotoxicity. Some of the compounds like **15d**, **15h**, **15k**, **15o**, **21d**, **21h**, **21k** and **21n** that possess difluoro substituents on the C-ring showed minimum cytotoxicity. Finally, it is observed that the presence of more methoxy groups on the C-ring increases the cytotoxicity, indicating that electron donating groups are important for the activity compared to electron withdrawing groups (OMe > F_2), however change of substitutions on the A-ring evidently plays a critical role towards the activity. Based on the structure–activity relationship, the optimal order of the substitution effect on the A-ring is trimethoxy > dimethoxy ≥ 3,4-(methylenedioxy) > monomethoxy (Fig. 2).[24,28,29]

Effect on cell morphology. Since these compounds (**15a**, **15b** and **15e**) demonstrated potent cytotoxicity it was neccesary to understand their effects on the cell morphology. Phase

10164 | *Org. Biomol. Chem.*, 2015, **13**, 10162–10178

This journal is © The Royal Society of Chemistry 2015

Table 1 Structures and IC$_{50}$ (μM) values of the synthesized compounds on HeLa,[b] DU-145,[c] MDA-MB231[d] and A549[e] cells determined by the MTT assay

Com	X	R^1	R^2	R^3	R^4	R^5	R^6	IC$_{50}$ values[a] (μM)			
								HeLa[b]	DU-145[c]	MDA-MB231[d]	A549[e]
15a	NH	OMe	OMe	OMe	OMe	OMe	OMe	0.4 ± 0.06	1.6 ± 0.13	1.0 ± 0.03	1.7 ± 0.05
15b	NH	OMe	OMe	OMe	OMe	OMe	H	1.8 ± 0.13	2.4 ± 0.15	2.6 ± 0.11	2.2 ± 0.12
15c	NH	OMe	OMe	OMe	H	OCH$_3$	H	3.5 ± 0.25	4.8 ± 0.9	5.6 ± 0.23	6.4 ± 0.18
15d	NH	OMe	OMe	OMe	F	F	H	13.7 ± 1.1	12.3 ± 0.5	19.2 ± 1.1	15.7 ± 1.0
15e	NH	OMe	OMe	H	OMe	OMe	OMe	1.2 ± 0.12	1.8 ± 0.19	1.6 ± 0.17	2.2 ± 0.10
15f	NH	OMe	OMe	H	OMe	OMe	H	5.5 ± 0.18	11 ± 0.2	13.2 ± 1.2	10.7 ± 0.3
15g	NH	OMe	OMe	H	H	OMe	H	10.4 ± 0.03	22.7 ± 1.7	36.5 ± 1.5	13.3 ± 0.5
15h	NH	OMe	OMe	H	F	F	H	14.2 ± 0.6	23.5 ± 1.5	14.2 ± 1.1	22.1 ± 1.0
15i	NH	H	OMe	H	OMe	OMe	OMe	2.7 ± 0.33	6.8 ± 0.4	3.8 ± 0.6	7.0 ± 0.8
15j	NH	H	OMe	H	OMe	OMe	H	13.5 ± 0.5	18.8 ± 0.9	15.6 ± 0.8	15.2 ± 1.2
15k	NH	H	OMe	H	F	F	H	16.1 ± 1.3	18.9 ± 0.2	15.4 ± 1.0	23.4 ± 1.1
15l	NH	–OCH$_2$O–		H	OCH$_3$	OCH$_3$	OCH$_3$	1.7 ± 0.18	1.9 ± 0.14	2.3 ± 0.28	2.9 ± 0.1
15m	NH	–OCH$_2$O–		H	OCH$_3$	OCH$_3$	H	12.2 ± 0.9	12.1 ± 0.1	17.8 ± 1.0	20.3 ± 1.2
15n	NH	–OCH$_2$O–		H	H	OCH$_3$	H	13.4 ± 1.1	3.1 ± 0.70	17.2 ± 1.7	9.7 ± 0.12
15o	NH	–OCH$_2$O–		H	F	F	H	29.7 ± 0.7	19.2 ± 1.12	23.1 ± 0.6	18.7 ± 1.1
21a	O	OMe	OMe	OMe	OMe	OMe	OMe	2.9 ± 0.16	3.2 ± 0.10	1.8 ± 0.11	4.3 ± 0.5
21b	O	OMe	OMe	OMe	OMe	OMe	H	3.7 ± 0.12	2.8 ± 0.38	2.5 ± 0.3	5.9 ± 0.2
21c	O	OMe	OMe	OMe	H	OMe	H	12.3 ± 0.1	14.2 + 0.3	22.1 ± 1.5	23.8 ± 1.1
21d	O	OMe	OMe	OMe	F	F	H	17.3 ± 1.5	21.8 ± 0.3	27.8 ± 0.9	25.6 ± 1.2
21e	O	OMe	OMe	H	OMe	OMe	OMe	3.3 ± 0.2	4.4 ± 0.5	2.3 ± 0.4	4.2 ± 0.6
21f	O	OMe	OMe	H	OMe	OMe	H	13.8 ± 1.0	15.8 ± 0.9	18.0 ± 1.9	10.7 ± 0.7
21g	O	OMe	OMe	H	H	OMe	H	20.1 ± 0.6	22.3 ± 0.4	19 ± 0.6	13.9 ± 0.5
21h	O	OMe	OMe	H	F	F	H	31.9 ± 0.7	28.0 ± 1.9	32.7 ± 1.7	22.1 ± 1.0
21i	O	H	OMe	H	OMe	OMe	OMe	5.4 ± 0.1	6.1 ± 0.6	3.8 ± 0.05	10.0 ± 0.6
21j	O	H	OMe	H	OMe	OMe	H	20.1 ± 0.6	39.8 ± 1.1	15.8 ± 0.8	10.2 ± 0.3
21k	O	H	OMe	H	F	F	H	34.9 ± 0.7	25.6 ± 1.3	28.9 ± 0.9	13.4 ± 0.1
21l	O	–OCH$_2$O–		H	OMe	OMe	OMe	4.2 ± 0.1	6.2 ± 0.21	4.9 ± 0.12	3.9 ± 0.7
21m	O	–OCH$_2$O–		H	OMe	OMe	H	20.1 ± 0.6	19.9 ± 1.6	11.2 ± 0.9	20.9 ± 1.6
21n	O	–OCH$_2$O–		H	F	F	H	19.8 ± 0.7	31.2 ± 1.7	22.1 ± 1.0	29.7 ± 1.2
Noc	—	—		—	—	—	—	0.5 ± 0.02	1.1 ± 0.03	0.7 + 0.03	0.9 + 0.04

[a] Each data represent mean + S.D. from three different experiments performed in triplicate. [b] HeLa: human cervix cancer cell line. [c] DU-145: human prostate cancer cell line. [d] MDA-MB231: human breast carcinoma cell line. [e] A549: human lung adenocarcinoma epithelial cell.
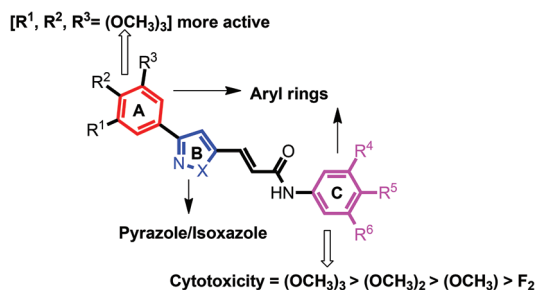

Fig. 2 SAR of pyrazole/isoxazole linked arylcinnamides. The compounds with a trimethoxy aryl group as the A-ring were comparatively more potent in the series. C-ring with more electropositive units enhances the cytotoxicity.

contrast images were observed to elucidate the morphology of cells treated with these compounds. Interestingly, HeLa cells treated by these compounds at 2 μM concentration manifested a rounded morphology similar to mitotic arrested cells. These results suggest that the possible mode of action for them is through the inhibition of mitosis (Fig. 3).

Effect on cell cycle arrest. Since the compound treated cells showed a predominant mitotic phenotype, we examined whether the cytoxicity induced by these derivatives was due to cell cycle arrest. Thus we performed flow cytometry analysis for the compounds that exhibited potent cytotoxicity HeLa cells were treated with 2 μM concentration of **15a**, **15b** and **15e** for 24 h. Cells treated with **15a** at 2 μM showed 75.53% arrest of cells in the G2/M phase, whereas **15b** and **15e** resulted in an
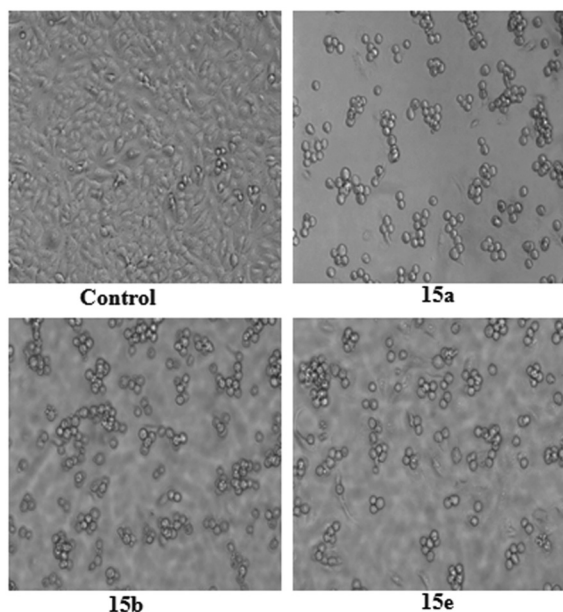
Fig. 3 Morphological representation of HeLa cells in the presence of the most active compounds: HeLa cells were treated with 2 μM of **15a**, **15b** and **15e** for 24 h. There is an abnormal cellular morphology noticed in compound treated cells indicating antiproliferative effects. DMSO was employed as negative control and such morphological abnormality was not observed.
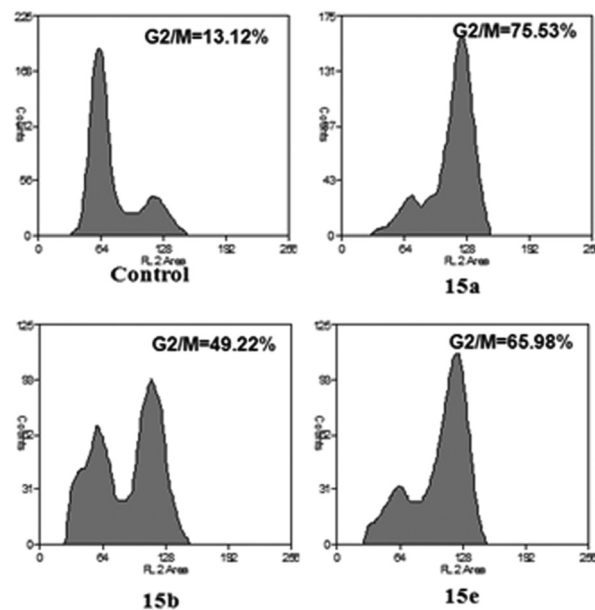

Fig. 4 Anti-mitotic effects of **15a**, **15b** and **15e** by FACS analysis: induced G2/M cell cycle arrest by compounds **15a**, **15b** and **15e**. HeLa cells were harvested after treatment at 2 μM for 24 h. Untreated cells and DMSO treated cells taken as controls. The percentage of cells in each phase of the cell cycle was measured quantitatively by flow cytometry.

increase of mitotic cell arrest by 49.22% and 65.98% respectively (Fig. 4).

Effect on tubulin polymerization. These pyrazole/isoxazole linked arylcinnamide conjugates were examined for their ability to inhibit tubulin polymerization as they exhibit potential cytotoxicity. Therefore, we incubated tubulin with varying concentrations of these conjugates to determine IC_{50} values for tubulin depolymerization activity and results are shown in Table 2. All the examined conjugates inhibit the polymerization of tubulin. Conjugate **15a** induces tubulin depolymerization significantly (IC_{50} value of 1.5 μM), whereas **15b** and **15e** inhibit tubulin assembly with IC_{50} values of 3.2 μM and 2.6 μM respectively (Table 2).

Effect on the microtubule network. The presence of anomalous spindle fibres due to disrupted microtubule dynamics is a hallmark of cells treated with antimitotic agents.[30] In order to ascertain whether the cell cycle arrest is due to spindle abnormality, HeLa cells were treated with 2 μM concentrations of these conjugates (**15a**, **15b** and **15e**) and stained with the tubulin antibody, whereas the control treated cells exhibit an organized network of microtubules. In contrast cells exposed to **15a** and **15b** showed multipolar spindle fibres, and **15e** treated cells exhibited a metaphase arrest (Fig. 5).

Effect on cellular tubulin polymerization and cyclin-B1. These observations suggest that the aberrant spindle dynamics in cells treated with **15a**, **15b** and **15e** result in cell cycle arrest. Tubulin assembly assays reveal that the congeners inhibit microtubule polymerization, consequently we analyzed

Table 2 Tubulin polymerization inhibitory effect of compounds **15a**, **15b** and **15e**

Compound	IC_{50} in μM
15a	1.5 ± 0.11
15b	3.2 ± 0.23
15e	2.6 ± 0.15
Nocodazole	0.87 ± 0.02

Effect of congeners on tubulin polymerization. IC_{50} values for **15a**, **15b** and **15e** were determined from the tubulin polymerization assay. Nocodazole was employed as positive control.

their effect on cellular tubulin. To elucidate this, HeLa cells were treated with these compounds at 2 μM concentration for 24 h.

Subsequently, cells were permeabilized to collect the soluble fraction and the remaining cells were collected as the polymerized fraction. Immunoblot analysis revealed that the cells exposed to pyrazole/isoxazole linked arylcinnamide conjugates restrained more tubulin in the soluble fraction. Therefore, increased tubulin in soluble fraction of cells treated with potent conjugates corroborated with the inhibition of tubulin assembly and arrest of cells in the G2/M phase of the cell cycle (Fig. 6).

To further authenticate our observations whether the pyrazole/isoxazole arylcinnamides function as potent tubulin polymerization inhibitors, HeLa cells were treated with the
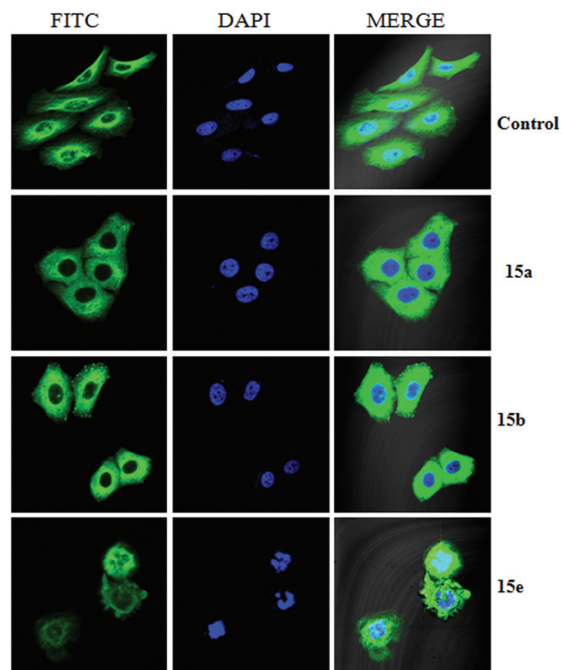
10166 | *Org. Biomol. Chem.*, 2015, **13**, 10162–10178

This journal is © The Royal Society of Chemistry 2015

Fig. 5 Effect on microtubules and nuclear condensation: HeLa cells were independently treated with **15a**, **15b** and **15e** at 2 μM concentration for 24 h. Following the termination of the experiment, cells were fixed and stained for tubulin. DAPI was used as counter stain. The merged images of cells stained for tubulin and DAPI are represented.
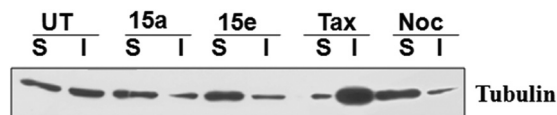

Fig. 6 Distribution of tubulin in soluble *vs.* insoluble fractions: HeLa cells were treated with 2 μM of **15a** and **15e** for 24 h. This image shows soluble and insoluble (polymerized) fractions of tubulin for **15a** and **15e**. A more soluble fraction is observed in **15a** treated cells when compared to **15e**. Nocodazole and Taxol were employed as reference standards. The amount of tubulin was detected by western blot analysis.

representative analogues **15a** and **15e** to demonstrate the elevated amount of cyclin B1 protein, a well recognized G2/M marker (Fig. 7). In addition, we further substantiated our results by performing semi-quantitative RT-PCR analysis for cyclin B1 mRNA levels in compounds **15a** and **15e** treated HeLa cells. Notably, treatments with the congeners showed a profound increase in cyclin B1 mRNA levels compared to control. Thus our results support the suggestion that the pyrazole/isoxazole arylcinnamides function as potent tubulin inhibitors that cause an accumulation of cells at the G2/M phase of the cell cycle (Fig. 8).

Molecular modeling studies. Molecular docking studies were also performed for the selected compounds like **15a** and **15b** to authenticate the obtained experimental results. These compounds were succesfully docked in the colchicine binding
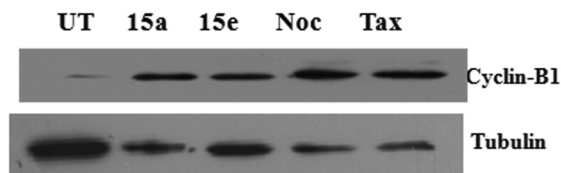

Fig. 7 Western blot analysis for cyclin-B1: HeLa cells were treated with 2 μM concentration of compounds **15a** and **15e** for 24 h. Subsequently, whole lysates were prepared and analyzed for cyclin-B1. Results illustrate an increased level of cyclin B1 in the treatments. The potent compound **15a** shows a pronounced expression of cyclin B1 levels. Tubulin was employed as loading control. Nocodazole (Noc) and taxol (Tax) were used as positive controls.
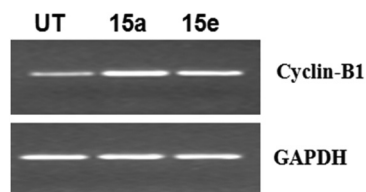

Fig. 8 RT-PCR analysis for cyclin B1 of the treated compounds **15a** and **15e**: HeLa cells treated with 2 μM concentration of compounds **15a** and **15e** for 24 h. Later, whole cell lysates were prepared and RNA was isolated. Semi-quantitative RT-PCR analysis was performed for cyclin-B1. GAPDH served as internal control.

site of the tubulin (PDB code: 3E22) by using the Autodock4 program.[31,32] Based on the previous reports it is well established that the colchicine site is commonly positioned at the interface of α and β protein heterodimers.[33] The conjugates upon docking are specifically surrounded by significant amino acid residues such as αSer-α178, αTyr-224, αVal-405, αTrp-407, αThr-223, and αAsn349 of the α subunit, βLeu-255, βLeu252, βCys-241, βGln-434 and βPhe-268, βThr-353, βPhe-343, βTyr-202, βAsn-258 and βAla-256 of the β subunit. The docking pose observed for **15a** showed a very similar binding to the cocrystallized DAMA-colchicine[34] with the trimethoxyphenyl ring (A-ring) in very close contact with βCys-241 (electrostatic interactions). However, the C-ring positioned in the binding pocket of the α subunit resulting the rest pyrazole bridge (B-ring) at the border of the two subunits. Additionally, the O atom of the unsaturated carbonyl structural unit forms a weak hydrogen bond with OH of αSer-178 (O···HO). Moreover, a weak hydrogen bond formed between the O atom of the trimethoxy group positioned at C3 of the C-ring, and NH of αThr-223 (O···HN). Significantly a strong hydrogen bond was observed between HN of the acrylamide linker and carbonyl O of βThr-353 of the β subunit (O···HN distance = 1.7 Å). Therefore, **15a** with trimethoxy benzene groups on both the A and C-rings occupies a similar position where colchicine binds to tubulin with little space orientation. However, superimposition poses explicate the important basic unit, a trimethoxy phenyl ring of both colchicine and **15a** occupy the exact location in the β subunit.
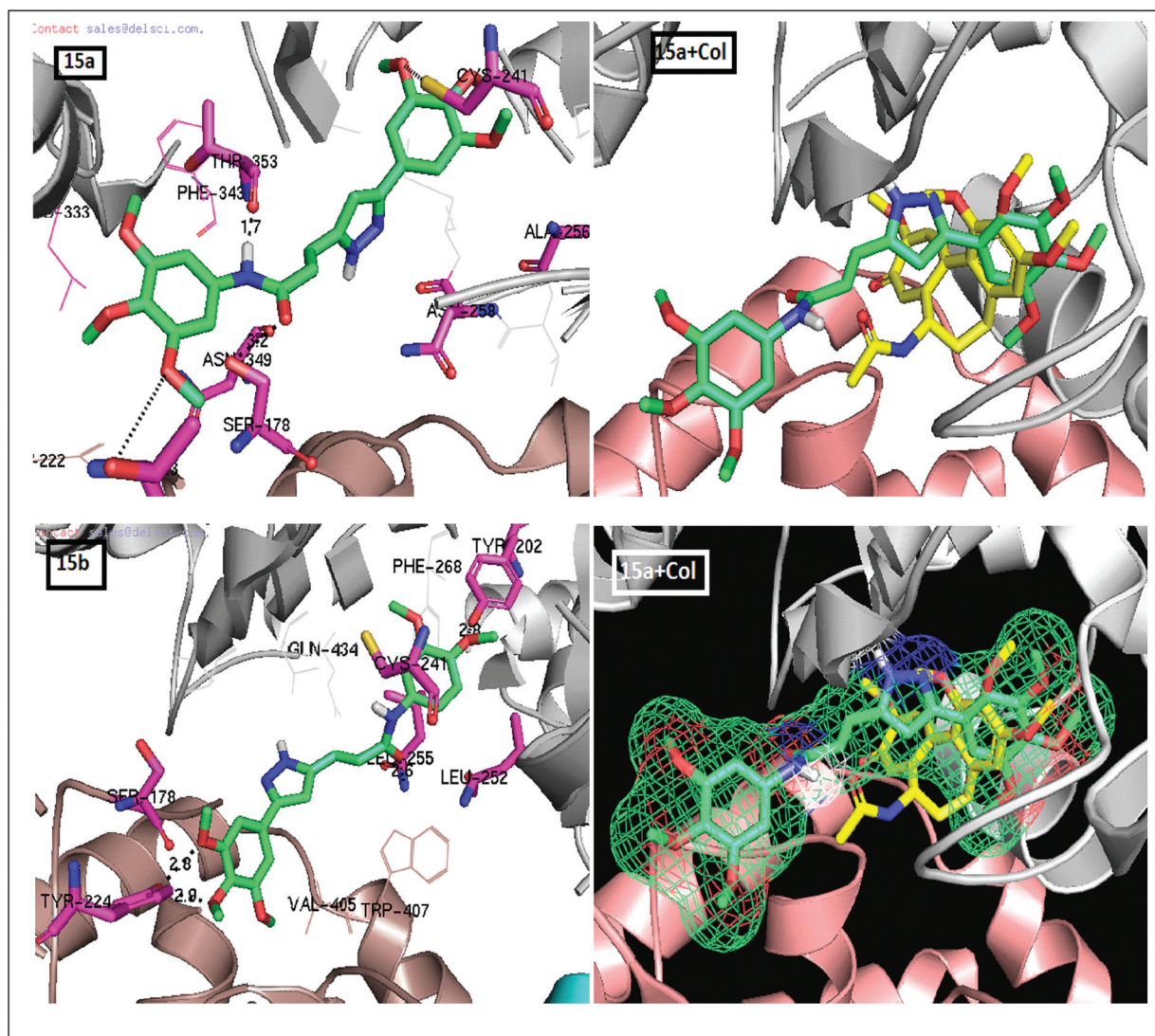
This journal is © The Royal Society of Chemistry 2015

Org. Biomol. Chem., 2015, **13**, 10162–10178 | **10167**

Fig. 9 Molecular modeling poses of the lead conjugates **15a**, **15b** and colchicine with **15a**: the panel of images represents the docking poses of the proposed ligands at the interface of α,β-tubulin. All the ligands are visualized in stick models (green color). The grey and salmon color ribbons depict α- and β-tubulin subunits respectively. The interacting residues that are shown in magenta stick model and potential inter molecular hydrogen bonding interactions were indicated with black dots. The poses (**15a+col**) represent **15a** along with colchicine occupy the same site in the tubulin. Images were generated with the PyMol programme.

The next tubulin polymerization inhibitor **15b** with a dimethoxy phenyl unit as the C-ring and the trimethoxy group on the A-ring is sandwiched between the two subunits showing strong hydrogen bonding with αTyr-224, and αTyr-202. In addition, a weak hydrogen bond is noted between the O atom of the dimethoxy group at the C3 position of the C-ring, and SH of βCys-241 (O···HS). Moreover, both the ligands exhibit few hydrophobic interactions with the residues like αVal-405, αTrp-407, αAsn349, βLeu-255, βLeu252, βGln-434, andβPhe-268, βPhe-343, βAsn-258 and βAla-256. Although the trimethoxy benzene group (A-ring) is identified as the signature for binding to tubulin, we noted that dimethoxy derivatives of **15b** inhibit the tubulin polymerization to a less extent than **15a**. These results are in accordance with the observed

experimental results; in particular, methoxy groups placed in a tight hydrophobic region at the interface of α and β heterodimers (Fig. 9).

Conclusions

In summary, we synthesized a new class of pyrazole/isoxazole linked arylcinnamide conjugates and investigated their antiproliferative activity against a panel of five cancer cell lines. These conjugates comprised a three ring molecular scaffold; A, B and C rings and these rings were decorated with various substitutions to present a comprehensive structure–activity relationship. Most of the compounds displayed significant

10168 | *Org. Biomol. Chem.*, 2015, **13**, 10162–10178

This journal is © The Royal Society of Chemistry 2015

cytotoxic activity wherein the presence of a trimethoxy phenyl group on the A-ring as well as C-rings was necessary for the tubulin inhibitory activity. Some of the promising compounds like **15a**, **15b** and **15e** inhibited the growth of cells in the G2/M phase and blocked the chromosomal translocation as well. The presence of increased levels of the cyclin B1 protein and tubulin in the soluble fraction of cells corroborate well with the tubulin polymerization inhibition. A significant upregulation of cyclin B1 mRNA by **15a** and **15e** indicates the activation of a cell cycle dependent apoptotic pathway as the mechanism of their cytotoxic effects. Molecular modeling analysis demonstrated that the compounds showed significant interactions to the colchicine binding site of tubulin. Based on the results, the design and synthesis of the compounds containing a pyrazole/isoxazole moiety are effective tubulin polymerization inhibitors, which can be further amenable for the generation of different conjugates as potential anticancer drugs.

Experimental section

General

All the chemicals and reagents used in this study were purchased from Aldrich (Sigma-Aldrich, St. Louis, MO, USA), Lancaster (Alfa Aesar, Johnson Matthey Company, Ward Hill, MA, USA), or Spectrochem Pvt. Ltd (Mumbai, India) and were used as such without purification. The reactions were monitored by TLC performed on silica gel glass plates containing 60 GF-254, and visualized by using a UV light or iodine indicator. Column chromatography was performed using Merck 60–120 mesh silica gel. ^{1}H NMR spectra were recorded on Bruker UXNMR/XWIN-NMR (300 MHz) or Inova Varian-VXR-unity (400, 500 MHz) instruments. ^{13}C NMR spectra were recorded on a Bruker UXNMR/XWIN-NMR (75 MHz) instrument. Chemical shifts (δ) were expressed as ppm downfield from an internal standard TMS. ESI spectra were recorded on a Micro mass Quattro LC using ESI+ software with a capillary voltage of 3.98 kV and an ESI mode positive ion trap detector. High-resolution mass spectra (HRMS) were recorded on a QSTAR XL hybrid MS–MS mass spectrometer.

Melting points were determined with an electrothermal melting point apparatus, and are uncorrected.

General preparation of (E)-ethyl 3-(3-aryl-1H-pyrazol-5-yl)-acrylates 12a–d

The different pyrazole carbaldehydes (**11a–d**) used in this study were taken from our previous report.[23] To the each **11a–d** was added equimolar amount of (carbethoxymethylene)-triphenylphosphine, Ph$_3$PCHCO$_2$C$_2$H$_5$, C2-wittig reagent in toluene at room temperature and continued stirring for 3–4 h. After performing TLC toluene was evaporated and an appropriate amount of water was added. The crude compounds were extracted by ethyl acetate (50 ml × 4). The organic layer was dried on anhydrous Na$_2$SO$_4$ and ethyl acetate was evaporated to obtain the corresponding pure α,β-unsaturated pyrazole esters (**12a–d**) in good yields (70–75%).

(E)-Ethyl 3-(3-(3,4,5-trimethoxyphenyl)-1H-pyrazol-5-yl)acrylate 12a. This compound was prepared by the addition of 3-(3,4,5-trimethoxyphenyl)-1H-pyrazole-5-carbaldehyde **11a** (262 mg 1.0 mmol) and Ph$_3$PCHCO$_2$C$_2$H$_5$ (248 mg, 1.0 mmol). Yellow solid (242 mg, yield 73%): R_f = 0.4 (30% ethyl acetate/hexane); ^{1}H NMR (300 MHz, CDCl$_3$); δ 1.33 (t, 3H, J = 7.1 Hz, –CH$_3$), 3.92 (s, 3H, –OCH$_3$), 3.93 (s, 6H, –OCH$_3$), 4.15–4.33 (q, 2H, J_1 = 7.0 Hz, J_2 = 7.1 Hz, –CH$_2$), 6.42 (d, 1H, transH J = 16.2 Hz), 6.72 (s, 1H, ArH), 6.92 (d, 1H, J = 8.6 Hz, ArH), 6.42 (d, 1H, transH J = 16.2 Hz), 7.17–7.23 (m, 1H, ArH) ppm; ^{13}C NMR (75 MHz, CDCl$_3$): 14.2, 56.0, 60.8, 101.9, 102.9, 119.1, 126.5, 128.4, 128.5, 131.6, 131.9, 132.0, 132.4, 134.1, 138.0, 153.4, 166.8 ppm; MS (ESI) m/z 333 [M + H]; HR-MS (ESI) m/z for C$_{17}$H$_{21}$O$_5$N$_2$ calculated m/z: 333.1405, found m/z: 333.1408.

(E)-Ethyl 3-(3-(3,4-dimethoxyphenyl)-1H-pyrazol-5-yl)acrylate 12b. This compound was prepared by the addition of 3-(3,4-dimethoxyphenyl)-1H-pyrazole-5-carbaldehyde **11b** (232 mg 1.0 mmol) and Ph$_3$PCHCO$_2$C$_2$H$_5$ (248 mg, 1.0 mmol). Yellow solid (217 mg, yield 72%): R_f = 0.5 (30% ethyl acetate/hexane); ^{1}H NMR (300 MHz, CDCl$_3$); δ 1.34 (t, 3H, J = 7.1 Hz, –CH$_3$), 3.94 (s, 3H, –OCH$_3$), 3.95 (s, 3H, –OCH$_3$), 4.10–4.31 (q, 2H, J_1 = 7.0 Hz, J_2 = 7.1 Hz, –CH$_2$), 6.12 (d, 1H, transH J = 16.1 Hz), 6.42 (d, 1H, transH J = 16.0 Hz), 6.74 (s, 2H, ArH), 7.19–7.21 (m, 2H, ArH) ppm; ^{13}C NMR (75 MHz, CDCl$_3$): 12.1, 53.7, 58.7, 94.4, 106.8, 109.7, 116.9, 117.4, 123.8, 129.3, 147.1, 148.8, 158.1, 163.2, 168.2 ppm; MS (ESI) m/z 303 [M + H]; HR-MS (ESI) m/z for C$_{16}$H$_{19}$O$_4$N$_2$ calculated m/z: 303.1305, found m/z: 303.1312.

(E)-Ethyl 3-(3-(4-methoxyphenyl)-1H-pyrazol-5-yl)acrylate 12c. This compound was prepared using the above-mentioned method by the addition of 3-(4-methoxyphenyl)-1H-pyrazole-5-carbaldehyde **11c** (202 mg 1.0 mmol) and Ph$_3$PCHCO$_2$C$_2$H$_5$ (248 mg, 1.0 mmol). Yellow solid (204 mg, yield 75%): R_f = 0.5 (30% ethyl acetate/hexane); ^{1}H NMR (300 MHz, CDCl$_3$); δ 1.29 (t, 3H, J = 7.1 Hz, –CH$_3$), 3.95 (s, 3H, –OCH$_3$), 4.08–4.23 (q, 2H, J_1 = 7.0 Hz, J_2 = 7.1 Hz, –CH$_2$), 6.32 (d, 1H, transH J = 16.1 Hz), 6.50 (s, 2H, ArH), 6.96 (d, 1H, J = 8.6 Hz, ArH), 6.65 (d, 1H, transH J = 16.2 Hz), 7.34–7.40 (m, 2H, ArH) ppm; ^{13}C NMR (75 MHz, CDCl$_3$): 13.9, 55.0, 60.7, 95.2, 114.1, 119.3, 125.1, 127.1, 128.9, 131.5, 159.8, 161.0, 165.3, 170.4 ppm; MS (ESI) m/z 273 [M + H]; HR-MS (ESI) m/z for C$_{15}$H$_{17}$O$_3$N$_2$ calculated m/z: 273.1148, found m/z: 273.1150.

(E)-ethyl 3-(3-(benzo[d][1,3]dioxol-5-yl)-1H-pyrazol-5-yl)acrylate 12d. This compound was prepared by the addition of 3-(benzo[d][1,3]dioxol-5-yl)-1H-pyrazole-5-carbaldehyde **11d** (216 mg 1.0 mmol) and Ph$_3$PCHCO$_2$C$_2$H$_5$ (248 mg, 1.0 mmol). Yellow solid (208 mg, yield 73%): R_f = 0.4 (30% ethyl acetate/hexane); ^{1}H NMR (300 MHz, CDCl$_3$); δ 0.85 (t, 3H, J = 7.3 Hz, –CH$_3$), 4.13–4.30 (q, 2H, J_1 = 5.3 Hz, –CH$_2$), 6.02 (s, 2H, –OCH$_2$O–), 6.45 (d, 1H, transH J = 15.8 Hz), 6.74–6.91 (m, 1H, ArH), 6.92 (d, 1H, J = 8.6 Hz, ArH), 7.06–7.32 (m, 2H, ArH), 7.56 (d, 1H, transH J = 15.8 Hz) ppm; ^{13}C NMR (75 MHz, CDCl$_3$): 12.7, 58.7, 99.6, 100.2, 104.3, 107.0, 117.3, 117.0, 123.4, 126.5, 130.8, 132.8, 139.2, 142.9 ppm; MS (ESI) m/z 287 [M + H]; HR-MS (ESI) m/z for C$_{15}$H$_{15}$O$_4$N$_2$ calculated m/z: 287.0988, found m/z: 287.0985.

This journal is © The Royal Society of Chemistry 2015

Org. Biomol. Chem., 2015, **13**, 10162–10178 | **10169**

Preparation of (*E*)-3-(3-phenyl-1*H*-pyrazol-5-yl)acrylic acid 13a–d

To each of the α,β-unsaturated pyrazole esters (**12a–d**) obtained in the above step was added equimolar lithium hydroxide (LiOH·H$_2$O) to a mixture of solvents THF : MeOH : H$_2$O (3 : 1 : 1) at room temperature and continued stirring for 3–4 h. After performing TLC the solvent mixture was evaporated and an appropriate amount of water was added. The crude compounds were extracted by ethyle acetate (50 ml × 4). The individual part of the aqueous layer was acidified using dil. HCl and then extracted by ethyl acetate (50 ml × 4) once again. The organic layer was dried on anhydrous Na$_2$SO$_4$ and then ethyl acetate was evaporated to obtain the corresponding pure (*E*)-3-(3-phenyl-1*H*-pyrazol-5-yl)acrylic acids (**13a–d**) in good yields (80–85%).

General procedure for synthesis of pyrazole linked arylcinnamides 15a–o

To the (*E*)-3-(3-phenyl-1*H*-pyrazol-5-yl)acrylic acid (**13a–d**) prepared in the above step was added equimolar EDCI (1-ethyl-3-(3-dimethylaminopropyl)carbodiimide) and a catalytic amount of Hobt (hydroxybenzotriazole) in ice cold dichloromethane. After 10 min appropriate amounts of aryl amines **14a–d** at 0 °C were added and stirring was continued at room temperature for 8 h. The progress of the reaction was monitored by TLC. After completion of the reaction an appropriate amount of sodium bicarbonate (NaHCO$_3$) solution was added and subsequently the final compounds were extracted with ethyl acetate (50 ml × 4). The organic layers so obtained were washed with 5% HCl solution and the organic solvent was evaporated, affording crude compounds. Further these compounds were purified using column chromatography by using an ethyl acetate and hexane solvent system to get pure compounds in good yields (60–80%).

(*E*)-*N*-(3,4,5-Trimethoxyphenyl)-3-(3-(3,4,5-trimethoxyphenyl)-1*H*-pyrazol-5-yl)acrylamide 15a. This compound was prepared by the addition of (*E*)-3-(3-(3,4,5-trimethoxyphenyl)-1*H*-pyrazol-5-yl)acrylic acid (304 mg 1.0 mmol) (**13a**) and 3,4,5-trimethoxyaniline (183 mg, 1.0 mmol) (**14a**). The compound was obtained as a pale yellow solid yield: 285 mg (60%); mp: 175–177 °C; ^{1}H NMR (300 MHz, CDCl$_3$ + DMSO-d$_6$); δ 3.80 (s, 6H, –OCH$_3$), 3.91 (s, 6H, –OCH$_3$), 3.96 (s, 6H, –OCH$_3$), 6.70 (s, 1H, –NH), 6.76 (d, 1H, *J* = 15.8 Hz, *trans*H), 6.85 (d, 1H, Ar**H**), 6.94 (d, 1H, Ar**H**), 7.35 (s, 1H *trans***H** *J* = 15.8 Hz) 7.51–7.57 (m, 1H, Ar**H**) 7.60–7.68 (m, 1H, Ar**H**), 9.54 (brs, 1H, –N**H**); ^{13}C NMR (75 MHz, CDCl$_3$ + DMSO-d$_6$): δ 54.1, 58.3, 100.8, 107.8, 117.1, 117.7, 125.1, 122.5, 126.0, 135.6, 140.9, 151.4, 165.8 ppm; IR (KBr) (ν_{max}/cm^{-1}): ν = 3235, 2938, 1695, 1623, 1592, 1500, 1462, 1427, 1368, 1246, 1129, 1086, 977 cm^{-1}; MS (ESI) *m/z* 471 [M + H]; HR-MS (ESI) *m/z* for C$_{24}$H$_{28}$O$_7$N$_2$ calculated *m/z*: 470.1849, found *m/z*: 470.1850.

(*E*)-*N*-(3,4-Dimethoxyphenyl)-3-(3-(3,4,5-trimethoxyphenyl)-1*H*-pyrazol-5-yl)acrylamide 15b. This compound was prepared by the addition of **13a** (304 mg, 1.0 mmol) and 3,4-dimethoxyaniline (**15b**) (153 mg 1.0 mmol). Colorless solid, yield: 276 mg (62%); mp: 191–193 °C; ^{1}H NMR (500 MHz,

CDCl$_3$ + DMSO-d$_6$); δ 3.86 (s, 6H, –OCH$_3$), 3.96 (s, 9H, –OCH$_3$), 7.01 (s, 1H, Ar**H**), 7.07 (s, 1H, Ar**H**), 7.55 (s, 1H, Ar**H**), 7.58–7.68 (m, 1H, –Ar**H**), 7.72 (d, 1H, *trans***H**, *J* = 15.8 Hz), 7.85 (t, 1H, Ar**H**, *J* = 7.3 Hz), 8.03 (d, 1H, Ar**H**, *J* = 8.4 Hz), 8.08 (d, 1H, *trans***H**, *J* = 15.6 Hz), 8.55 (brs, 1H, –N**H**) ppm; ^{13}C NMR (75 MHz, CDCl$_3$ + DMSO-d$_6$): 58.6, 95.4, 99.1, 107.2, 108.1, 109.9, 116.2, 120.8, 122.8, 124.6, 126.9, 130.0, 131.9, 133.8, 147.1, 147.2, 151.0, 162.0 IR (KBr) (ν_{max}/cm^{-1}): ν = 3253, 2932, 2926, 1693, 1622, 1589, 1460, 1460, 1426, 1342, 1084, 971 cm^{-1}; MS (ESI) *m/z* 440 [M + H]; HR-MS (ESI) *m/z* for C$_{23}$H$_{26}$O$_6$N$_3$ calculated *m/z*: 440.1823, found *m/z*: 440.1823.

(*E*)-*N*-(4-Methoxyphenyl)-3-(3-(3,4,5-trimethoxyphenyl)-1*H*-pyrazol-5-yl)acrylamide 15c. This compound was prepared by the addition of **13a** (304 mg, 1.0 mmol) and 4-methoxyaniline **14c** (123 mg 1.0 mmol). Pale yellow solid, yield: 285 mg (69%); mp: 208–210 °C; ^{1}H NMR (300 MHz, CDCl$_3$ + DMSO-d$_6$); δ 3.79 (s, 3H, –OCH$_3$), 3.81 (s, 3H, –OCH$_3$), 3.92 (s, 6H, –OCH$_3$), 6.78 (d, 1H, *trans***H**, *J* = 15.6 Hz), 6.85 (d, 1H, Ar**H**, *J* = 8.8 Hz), 7.05 (s, 3H, Ar**H**), 7.57 (d, 1H, *trans***H**, *J* = 15.8 Hz), 7.64 (d, 1H, Ar**H**, *J* = 8.6 Hz), 7.83 (s, 2H, Ar**H**, *J* = 8.6 Hz), 9.88 (brs, 1H, –N**H**) ppm; ^{13}C NMR (75 MHz, CDCl$_3$ + DMSO-d$_6$): 53.6, 54.4, 58.6, 100.0, 100.1, 112.3, 119.5, 121.2, 130.4, 135.5, 151.6, 153.9, 161.9 ppm; IR (KBr) (ν_{max}/cm^{-1}): ν = 3422, 3061, 3606, 2927, 1657, 1604, 1509, 1466, 1408, 1346, 1237, 1127, 1024, 1000, 968 cm^{-1}; MS (ESI) *m/z* 410 [M + H]; HR-MS (ESI) *m/z* for C$_{22}$H$_{24}$O$_5$N$_3$ calculated *m/z*: 410.1710, found *m/z*: 410.1731.

(*E*)-*N*-(3,4-Difluorophenyl)-3-(3-(3,4,5-trimethoxyphenyl)-1*H*-pyrazol-5-yl)acrylamide 15d. This compound was prepared by the addition of **13a** (304 mg 1.0 mmol) and 3,4-difluoroaniline **14d** (130 mg 1.0 mmol). Pale yellow solid, yield: 290 mg (70%); mp: 216–218 °C; ^{1}H NMR (300 MHz, CDCl$_3$ + DMSO-d$_6$); δ 3.82 (s, 3H, –OCH$_3$), 3.94 (s, 6H, –OCH$_3$), 6.75 (d, 2H, *J* = 15.8 Hz, *trans***H**), 7.05 (s, 1H, Ar**H**), 7.06–7.18 (m, 1H, Ar**H**), 7.36 (d, 1H, Ar**H** *J* = 9.2 Hz), 7.63 (d, 1H, *J* = 15.8 Hz, *trans***H**), 7.77 (s, 1H, Ar**H**), 7.83–7.94 (m, 1H, Ar**H**), 10.15 (brs, 1H, N**H**); ^{13}C NMR (75 MHz, CDCl$_3$ + DMSO-d$_6$): δ 54.2, 58.4, 99.8, 101.0, 106.8, 106.8, 107.8, 113.6, 11501, 11504, 120.3, 134.4, 135.8, 142.2, 151.5, 162.1 ppm; IR (KBr) (ν_{max}/cm^{-1}): ν = 3218, 2928, 1623, 1532, 1512, 1468, 1424, 1345, 1247, 1132, 1087, 996 cm^{-1}; MS (ESI) *m/z* 416 [M + H]; HR-MS (ESI) *m/z* for C$_{21}$H$_{20}$F$_2$O$_4$N$_3$ calculated *m/z*: 416.1419 found *m/z*: 416.1420.

(*E*)-3-(3-(3,4-Dimethoxyphenyl)-1*H*-pyrazol-5-yl)-*N*-(3,4,5-trimethoxyphenyl)acrylamide 15e. This compound was prepared by the addition of (*E*)-3-(3-(3,4-dimethoxyphenyl)-1*H*-pyrazol-5-yl)acrylic acid **13b** (274 mg 1.0 mmol) and 3,4,5-trimethoxyaniline **14a** (183 mg, 1.0 mmol). Pale yellow solid, yield: 310 mg (70%); mp: 204–206 °C; ^{1}H NMR (500 MHz, DMSO-d$_6$); δ 3.87 (s, 6H, –OCH$_3$), 3.96 (s, 12H, OCH$_3$), 7.01 (s, 1H, –Ar**H**), 7.07 (s, 1H, Ar**H**), 7.54 (s, 1H, Ar**H**), 7.60–7.68 (m, 1H, Ar**H**) 7.72 (d, 1H, *trans***H**, *J* = 15.6 Hz), 7.82–7.89 (m, 1H, Ar**H**), 8.09 (d, 1H, *trans***H**, *J* = 15.8 Hz), 8.54 (d, 1H, Ar**H**, *J* = 8.4 Hz), 9.67 (brs, 1H, N**H**), 13.03 (brs, 1H, NH); ^{13}C NMR (75 MHz, CDCl$_3$ + DMSO-d$_6$): δ 54.5, 58.7, 96.3, 100.2, 101.2, 108.0, 117.3, 117.9, 122.7, 125.2, 136.0, 151.7, 166.2 ppm; IR (KBr) (ν_{max}/cm^{-1}): ν = 3230, 3010, 1685, 1635, 1596, 1575, 1500, 1487, 1468, 1368, 1290, 1225, 1180, 1115,

10170 | *Org. Biomol. Chem.*, 2015, **13**, 10162–10178

This journal is © The Royal Society of Chemistry 2015

1026, 998 cm^{-1}; MS (ESI) m/z 440 [M + H]; HR-MS (ESI) m/z for C$_{23}$H$_{26}$O$_6$N$_3$ calculated m/z: 440.1816 found m/z: 440.1807.

(E)-N-(3,4-Dimethoxyphenyl)-3-(3-(3,4-dimethoxyphenyl)-1H-pyrazol-5-yl)acrylamide 15f. This compound was prepared by the addition of **13b** (274 mg, 1.0 mmol) and 3,4-dimethoxyaniline **14b** (153 mg 1.0 mmol). Yellow crystals, yield: 260 mg (68%); mp: 214–216 °C; ^{1}H NMR (500 MHz, CDCl$_3$ + DMSO-d$_6$); δ 3.87 (s, 3H, –OCH$_3$), 3.91 (s, 6H, –OCH$_3$), 3.95 (s, 3H, –OCH$_3$), 6.69 (s, 1H, Ar**H**), 6.72 (d, 1H, *trans***H**, J = 16.0 Hz), 6.82 (d, 1H, Ar**H**, J = 8.6 Hz), 6.91 (d, 1H, Ar**H**, J = 9.0 Hz), 7.33 (s, 3H, Ar**H**), 7.61 (s, 1H, Ar**H**), 7.66 (d, 1H, *trans***H**, J = 15.7 Hz), 8.99 (brs, 1H, –N**H**); ^{13}C NMR (75 MHz, DMSO-d$_6$): δ 54.0, 54.2, 54.4, 99.1, 103.1, 107.5, 110.0, 110.2, 116.5, 121.2, 131.6, 143.5, 147.3, 147.5, 147.3, 162.1, 165.5 ppm; IR (KBr) (ν_{max}/cm^{-1}): ν = 2934, 1660, 1510, 1463, 1339, 1234, 1169, 1026, 805 cm^{-1}; MS (ESI) m/z 410 [M + H].

(E)-3-(3-(3,4-Dimethoxyphenyl)-1H-pyrazol-5-yl)-N-(4-methoxyphenyl)acrylamide 15g. This compound was prepared by the addition of **13b** (274 mg, 1.0 mmol) and 4-methoxyaniline **14c** (123 mg 1.0 mmol). The compound was obtained as a colorless solid, yield: 290 mg (76%); mp: 228–230 °C; ^{1}H NMR (500 MHz, CDCl$_3$ + DMSO-d$_6$); δ 3.80 (s, 3H, –OCH$_3$), 3.91 (s, 3H, –OCH$_3$), 3.95 (s, 3H, –OCH$_3$), 6.72 (s, 1H, Ar**H**), 6.77 (d, 1H, J = 15.6 Hz, *trans***H**), 6.84 (s, 1H, Ar**H**), 6.89 (s, 1H, Ar**H**), 6.94 (d, 1H, J = 8.3 Hz, Ar**H**), 7.35 (d, 1H, *trans***H**, J = 16.2 Hz), 7.57–7.69 (m, 4H, Ar**H**), 8.72 (brs, 1H, –N**H**); ^{13}C NMR (75 MHz, CDCl$_3$ + DMSO-d$_6$): δ 54.4, 54.9, 100.1, 108.0, 110.6, 112.9, 117.2, 120.3, 121.9, 131.4, 147.9, 148.1, 154.8, 162.9 ppm; IR (KBr) (ν_{max}/cm^{-1}): ν = 3311, 3135, 2940, 2841, 1729, 1676, 1610, 1509, 1449, 1419, 1307, 1250, 1181, 1140, 995 cm^{-1}; MS (ESI) m/z 380 [M + H]; HR-MS (ESI) m/z for C$_{21}$H$_{22}$O$_4$N$_3$ calculated m/z: 380.1602 found m/z: 380.1614.

(E)-N-(3,4-Difluorophenyl)-3-(3-(3,4-dimethoxyphenyl)-1H-pyrazol-5-yl)acrylamide 15h. This compound was prepared by the addition of **13b** (274 mg, 1.0 mmol) and 3,4-difluoroaniline **14d** (130 mg 1.0 mmol). Yellow solid, yield: 300 mg (77%); mp: 188–189 °C; ^{1}H NMR (500 MHz, CDCl$_3$ + DMSO-d$_6$); δ 3.91 (s, 3H, –OCH$_3$), 3.96 (s, 3H, –OCH$_3$), 6.75 (d, 1H, *trans***H**, J = 15.6 Hz), 6.93 (d, 1H, Ar**H**, J = 8.3 Hz), 7.05–7.22 (m, 1H, Ar**H**), 7.29–7.41 (m, 2H, Ar**H**), 7.55 (s, 2H, Ar**H**), 7.65 (d, 1H, *trans***H**, J = 15.8 Hz), 7.81–7.93 (m, 1H, Ar**H**), 10.05 (brs, 1H, –N**H**); IR (KBr) (ν_{max}/cm^{-1}): ν = 3230, 3010, 1640, 1610, 1586, 1550, 1496, 1480, 1410, 1380, 1254, 1200, 1175, 1110, 1026, 993 cm^{-1}; MS (ESI) m/z 386 [M + H]; HR-MS (ESI) m/z for C$_{20}$H$_{18}$F$_2$O$_3$N$_3$ calculated m/z: 386.1338, found m/z: 386.1320.

(E)-3-(3-(4-Methoxyphenyl)-1H-pyrazol-5-yl)-N-(3,4,5-trimethoxyphenyl)acrylamide 15i. This compound was prepared by the addition of (E)-3-(3-(4-methoxyphenyl)-1H-pyrazol-5-yl)acrylic acid **13c** (244 mg 1.0 mmol) and 3,4,5-trimethoxyaniline **14a** (183 mg, 1.0 mmol). Yellow solid, yield: 298 mg (73%); mp: 208–210 °C; ^{1}H NMR (500 MHz, CDCl$_3$ + DMSO-d$_6$); δ 3.76 (s, 3H, –OCH$_3$), 3.85 (s, 9H, –OCH$_3$), 6.75 (d, 1H, *trans***H**, J = 15.4 Hz), 6.78 (s, 1H, Ar**H**), 6.96 (d, 2H, J = 8.4 Hz, Ar**H**), 7.12 (s, 2H, Ar**H**), 7.59 (d, 1H, *trans***H**, J = 15.6 Hz), 7.70 (d, 2H, Ar**H**, J = 8.4 Hz), 9.98 (brs, 1H, –N**H**); ^{13}C NMR (75 MHz, DMSO-d$_6$): δ 54.8, 55.4, 60.1, 96.8, 100.4, 113.7, 122.1, 123.2, 126.3, 130.3,

133.3, 135.0, 152.4, 158.8, 163.7 ppm; IR (KBr) (ν_{max}/cm^{-1}): ν = 3220, 3016, 2960, 1680, 1650, 1600, 1584, 1536, 1491, 1437, 1366, 1244, 1215, 1173, 1105, 1030, 985 cm^{-1}; MS (ESI) m/z 410 [M + H]; HR-MS (ESI) m/z for C$_{22}$H$_{24}$O$_5$N$_3$ calculated m/z: 410.1714, found m/z: 410.1713.

(E)-N-(3,4-Dimethoxyphenyl)-3-(3-(4-methoxyphenyl)-1H-pyrazol-5-yl)acrylamide 15j. This compound was prepared by the addition of **13c** (244 mg, 1.0 mmol) and 3,4-dimethoxyaniline **14b** (153 mg 1.0 mmol). Yellow solid, yield: 260 mg (68%); mp: 218–220 °C; ^{1}H NMR (300 MHz, CDCl$_3$ + DMSO-d$_6$); δ 3.78 (s, 6H, –OCH$_3$), 3.84 (s, 3H, –OCH$_3$), 6.19 (s, 1H, Ar**H**), 6.69 (s, 1H, Ar**H**), 6.75 (d, 1H, J = 15.6 Hz, *trans***H**), 6.91–6.97 (m, 3H, Ar**H**), 7.01 (s, 1H, Ar**H**), 7.62 (d, 1H, J = 15.4 Hz, *trans***H**), 7.66–7.74 (m, 2H, Ar**H**), 9.82 (brs, 1H, –N**H**); IR (KBr) (ν_{max}/cm^{-1}): ν = 3241, 3112, 3060, 1680, 1640, 1591, 1555, 1484, 1430, 1316, 1288, 1261, 1190, 1180, 1115, 1020, 987 cm^{-1}; MS (ESI) m/z 380 [M + H].

(E)-N-(3,4-Difluorophenyl)-3-(3-(4-methoxyphenyl)-1H-pyrazol-5-yl)acrylamide 15k. This compound was prepared by the addition of **13c** (244 mg, 1.0 mmol) and 3,4-difluoroaniline **14d** (130 mg 1.0 mmol). Yellow solid, yield: 310 mg (78%); mp: 214–216 °C; ^{1}H NMR (500 MHz, CDCl$_3$ + DMSO-d$_6$); δ 3.84 (s, 3H, –OCH$_3$), 6.73 (s, 1H, Ar**H**), 6.73 (d, 1H, J = 15.8 Hz *trans***H**), 6.95 (d, 2H, J = 8.3 Hz, Ar**H**), 7.07–7.20 (m, 1H, Ar**H**), 7.31–7.40 (m, 1H, Ar**H**), 7.61 (d, 1H, J = 15.6 Hz, *trans***H**), 7.69 (d, 2H, J = 8.3 Hz, Ar**H**), 6.73 (s, 1H, Ar**H**), 10.2 (brs, 1H, –N**H**); ^{13}C NMR (75 MHz, CDCl$_3$ + DMSO-d$_6$): δ 54.6, 95.4, 97.5, 100.3, 113.5, 122.0, 123.8, 126.2, 130.3, 130.9, 140.3, 158.8, 160.1 ppm; IR (KBr) (ν_{max}/cm^{-1}): ν = 3223, 3018, 2950, 1679, 1610, 1580, 1515, 1486, 1441, 1353, 1325, 1273, 1260, 1147, 1110, 1065, 998 cm^{-1}; MS (ESI) m/z 356 [M + H].

(E)-3-(3-(Benzo[d][1,3]dioxol-5-yl)-1H-pyrazol-5-yl)-N-(3,4,5-trimethoxyphenyl)acrylamide 15l. This compound was prepared by the addition of (E)-3-(3-(benzo[d][1,3]dioxol-5-yl)-1H-pyrazol-5-yl)acrylic acid **13d** (258 mg 1.0 mmol) and 3,4,5-trimethoxyaniline **14a** (183 mg, 1.0 mmol). Brown solid, yield: 310 mg (73%); mp: 198–200 °C; ^{1}H NMR (300 MHz, CDCl$_3$ + DMSO-d$_6$); δ 3.87 (s, 6H, –OCH$_3$), 3.70 (s, 3H, –OCH$_3$), 6.09 (s, 2H, –OCH$_2$O–), 6.97 (d, 1H, J = 15.8 Hz, *trans***H**), 7.12 (s, 1H, Ar**H**), 7.31–7.35 (m, 1H, Ar**H**), 7.37 (s, 1H, Ar**H**), 7.41 (d, 1H, J = 8.0 Hz, Ar**H**), 7.52 (d, 1H, J = 15.8 Hz, *trans***H**), 7.61 (d, 1H, J = 8.4 Hz, Ar**H**), 7.86 (d, 1H, J = 8.4 Hz, Ar**H**), 10.3 (brs, 1H, –N**H**); IR (KBr) (ν_{max}/cm^{-1}): ν = 3208, 2933, 1669, 1609, 1550, 1506, 1455, 1386, 1234, 1187, 1127, 1105, 1036, 975 cm^{-1}; MS (ESI) m/z 424 [M + H]; HR-MS (ESI) m/z for C$_{22}$H$_{22}$O$_6$N$_3$ calculated m/z: 424.1502, found m/z: 424.1502.

(E)-3-(3-(Benzo[d][1,3]dioxol-5-yl)-1H-pyrazol-5-yl)-N-(3,4-dimethoxyphenyl)acrylamide 15m. This compound was prepared by the addition of **13d** (258 mg, 1.0 mmol) and 3,4-dimethoxyaniline **14b** (153 mg 1.0 mmol). Pale yellow solid, yield: 280 mg (71%); mp: 180–182 °C; ^{1}H NMR (300 MHz, CDCl$_3$ + DMSO-d$_6$); δ 3.78 (s, 3H, –OCH$_3$), 3.80 (s, 3H, –OCH$_3$), 5.98 (s, 2H, –OCH$_2$O–), 6.22 (s, 1H, Ar**H**), 6.60–6.72 (m, 2H, Ar**H**, J = 15.8 Hz, *trans***H**), 6.84 (t, 1H, J = 8.2 Hz, Ar**H**), 6.95 (s, 2H, Ar**H**), 7.20–7.28 (m, 2H, Ar**H**), 7.63 (d, 1H, J = 15.5 Hz, *trans***H**), 8.87 (brs, 1H, –N**H**); ^{13}C NMR (75 MHz, CDCl$_3$ +

This journal is © The Royal Society of Chemistry 2015

Org. Biomol. Chem., 2015, **13**, 10162–10178 | **10171**

DMSO-d$_6$): δ 53.9, 96.8, 99.8, 104.7, 107.2, 117.9, 121.4, 130.6, 132.2, 139.6, 146.1, 146.7, 159.4 ppm; IR (KBr) (ν_{max}/cm^{-1}): ν = 3208, 2927, 1614, 1558, 1462, 1322, 1246, 1204, 1153, 1037, 972 cm^{-1}; MS (ESI) m/z 394 [M + H].

(E)-3-(3-(Benzo[d][1,3]dioxol-5-yl)-1H-pyrazol-5-yl)-N-(4-methoxyphenyl)acrylamide 15n. This compound was prepared by the addition of **13d** (258 mg, 1.0 mmol) and 4-methoxyaniline **14c** (123 mg 1.0 mmol). Brown solid, yield: 291 mg (80%); 196–198 °C; ^{1}H NMR (300 MHz, DMSO-d$_6$); δ 3.78 (s, 3H, –OCH$_3$), 6.02 (s, 2H, –OCH$_2$O–), 6.73 (s, 1H, ArH), 6.75 (d, 1H, ArH, J = 15.6 Hz, transH), 6.86 (t, 3H, J = 9.0 Hz, ArH), 7.21–7.34 (m, 2H, ArH), 7.52 (d, 1H, J = 15.6 Hz, transH), 7.63 (d, 2H, ArH, J = 8.8 Hz) 7.96 (brs, 1H, –NH); ^{13}C NMR (75 MHz, DMSO-d$_6$): δ 53.4, 99.4, 103.9, 106.8, 112.1, 117.4, 119.3, 121.0, 130.5, 145.4, 146.0, 153.7, 161.6 ppm; IR (KBr) (ν_{max}/cm^{-1}): ν = 3216, 3100, 3096, 1688, 1651, 1596, 1542, 1505, 1473, 1450, 1330, 1311, 1285, 1215, 1167, 1108, 1035, 998 cm^{-1}; MS (ESI) m/z 364 [M + H]; HR-MS (ESI) m/z for C$_{20}$H$_{18}$O$_4$N$_3$ calculated m/z: 364.1298, found m/z: 364.1298.

(E)-3-(3-(Benzo[d][1,3]dioxol-5-yl)-1H-pyrazol-5-yl)-N-(3,4-difluorophenyl)acrylamide 15o. This compound was prepared by the addition of **13d** (258 mg, 1.0 mmol) and 3,4-difluoroaniline **14d** (130 mg 1.0 mmol). Pale yellow solid, yield: 270 mg (73%); mp: 185–187 °C; ^{1}H NMR (300 MHz, CDCl$_3$ + DMSO-d$_6$); δ 6.03 (s, 2H, –OCH$_2$O–), 6.72 (d, 1H, ArH, J = 15.6 Hz, transH), 6.78 (s, 1H, ArH), 6.89 (d, 1H, J = 9.0 Hz, ArH), 7.12–7.43 (m, 4H, ArH), 7.55 (d, 1H, J = 15.6 Hz, transH), 7.83–7.96 (m, 1H, ArH), 8.06 (brs, 1H, –NH); ^{13}C NMR (75 MHz, CDCl$_3$+DMSO-d$_6$): δ 99.03, 103.9, 106.5, 106.7, 115.1, 113.6, 115.3, 117.2, 120.2, 134.5, 145.4, 146.0, 162.0 ppm; IR (KBr) (ν_{max}/cm^{-1}): ν = 3302, 3163, 3016, 1690, 1645, 1610, 1550, 1515, 1473, 1441, 1361, 1322, 1241, 1201, 1116, 1026, 979 cm^{-1}; MS (ESI) m/z 370 [M + H]; HR-MS (ESI) m/z for C$_{19}$H$_{14}$O$_3$N$_3$F$_2$ calculated m/z: 370.1003, found m/z: 370.1002.

Preparation of ethyl 3-substituted phenylisoxazole-5-carboxylates 16a–d

To each of the ethyl 2,4-dioxo-4-(substituted phenyl) butanoates **8(a–d)** (1.0 mol) which were obtained in the earlier step was added hydroxylamine hydrochloride (NH$_2$–OH·HCl) (1.5 mol) in ethanol and heated to reflux for 3 h. The solvent was removed under vacuum and then water was added to the residue and the compound was extracted with ethyl acetate (50 ml × 4). The organic layer was dried on anhydrous Na$_2$SO$_4$ and the solvent was evaporated to obtain the crude product that was further purified by column chromatography using ethyl acetate and hexane. The pure compounds **16(a–d)** were eluted at 20–25% ethyl acetate with good yields (75–80%).

Ethyl 3-(3,4,5-trimethoxyphenyl)isoxazole-5-carboxylate 16a. Pale yellow solid (yield 75.0%): R_f = 0.5 (20% ethyl acetate/hexane); ^{1}H NMR (300 MHz, CDCl$_3$); δ 1.45 (t, 3H, J = 7.1 Hz, –CH$_3$), 3.92 (s, 3H, –OCH$_3$), 3.93 (s, 6H, –OCH$_3$) 4.48 (q, 2H, J_1 = 7.0 Hz, –CH$_2$), 6.88 (s, 1H, ArH), 7.02 (s, 2H, ArH) ppm; MS (ESI) m/z 308 [M + H].

2 ethyl 3-(3,4-dimethoxyphenyl)isoxazole-5-carboxylate 16b. Pale yellow solid (yield 80.0%): R_f = 0.5 (15% ethyl acetate/hexane); ^{1}H NMR (300 MHz, CDCl$_3$); δ 1.21–1.31 (t, 3H, J = 7.4 Hz, –CH$_3$), 3.87 (s, 3H, –OCH$_3$), 3.94 (s, 3H, –OCH$_3$) 4.10–4.22 (q, 2H, J = 7.0 Hz, –CH$_2$), 6.85 (d, 1H, J = 7.2 Hz, –ArH), 6.97 (s, 1H, ArH), 7.23–7.27 (m, 1H, ArH) 7.30–7.33 (m, 1H, ArH) ppm; MS (ESI) m/z 278 [M + H].

Ethyl 3-(4-methoxyphenyl)isoxazole-5-carboxylate 16c. Yellow solid (yield 80%); R_f = 0.5 (15% ethyl acetate/hexane); ^{1}H NMR (500 MHz, CDCl$_3$); δ 1.23–1.37 (t, 3H, J = 6.7 Hz,–CH$_3$), 3.87 (s, 3H, –OCH$_3$), 4.15–4.35 (q, 2H, J_1 = 6.7 Hz, J_2 = 7.5 Hz, CH$_2$), 6.85 (s, 1H, ArH), 7.01 (d, 2H, J = 7.2 Hz, ArH), 7.68 (d, 2H, J = 8.9 Hz, ArH) ppm; MS (ESI) m/z 248 [M + H].

Ethyl 3-(benzo[d][1,3]dioxol-5-yl)isoxazole-5-carboxylate 16d. Pale yellow solid (yield 75.0%): R_f = 0.6 (30% ethyl acetate/ hexane); ^{1}H NMR (500 MHz, CDCl$_3$); δ 1.44 (t, 3H, J_1 = 7.1 Hz, –CH$_3$), 4.47 (q, 2H, J = 7.1 Hz, –CH$_2$), 5.98 (s, 2H, –OCH$_2$O), 6.79 (s, 1H, ArH), 6.81 (s, 1H, ArH), 6.86 (d, 1H, J = 7.1 Hz, ArH), 7.19 (s, 1H, ArH) ppm; MS (ESI) m/z 218 [M + H].

Preparation of (3-substituted phenylisoxazol-5-yl)methanol 17(a–d)

To the 3-substituted phenylisoxazole-5-carboxylates **16(a–d)**, obtained in the above step was added LiAlH$_4$ (0.5 mol) in dry THF at 0 °C and stirred for 1 h at room temperature. Saturated NH$_4$Cl solution was added dropwise to quench the unreacted LiAlH$_4$ and THF was removed under vacuum and then extracted with ethyl acetate (100 ml × 4). The organic layer was dried on anhydrous Na$_2$SO$_4$ and ethyl acetate was evaporated to obtain colorless solid products of (3-substituted phenyl-isoxazol-5-yl)methanols **17(a–d)** (yield 70–80%). The alcohols produced in this step were pure and taken as such for the next step.

Preparation of 3-substituted phenylisoxazole-5-carbaldehydes 18a–d

To each (3-substituted phenylisoxazol-5-yl) of the methanols **17(a–d)** produced in the above step was added IBX (1.2 mol) in DMSO and stirred for 1 h at room temperature. Ice cold water was added to the reaction mixture and extracted with ethyl-acetate (50 ml × 4). The organic layer was dried on anhydrous Na$_2$SO$_4$ and ethyl acetate was evaporated to obtain the corresponding pure 3-sustituted phenylisoxazole-5-carbaldehydes **18 (a–d)** in good yields (80–85%). The obtained carbaldehydes were taken as such in the next step.

3-(3,4,5-Trimethoxyphenyl)isoxazole-5-carbaldehyde 18a. This compound was prepared by the addition of (3-(3,4,5-trimethoxyphenyl)isoxazol-5-yl)methanol **17a** (2.62 g 10 mmol) and IBX (3.36 g 1.2 mmol). Yellow solid (2.13 g, yield 81%): R_f = 0.3 (40% ethyl acetate/hexane); ^{1}H NMR (400 MHz, CDCl$_3$); δ 3.89 (s, 3H, –OCH$_3$), 3.95 (s, 6H, –OCH$_3$), 6.96 (s, 1H, ArH), 7.08 (s, 2H, ArH), 10.18 (s, 1H, –CHO) ppm; MS (ESI) m/z 264 [M + H].

3-(3,4-Dimethoxyphenyl)isoxazole-5-carbaldehyde 18b. This compound was prepared by the addition of (3-(3,4-dimethoxyphenyl)isoxazol-5-yl)methanol **17b** (2.35 g 10 mmol) and IBX (3.36 g 1.2 mmol). Yellow solid (1.93 g, yield 83%): R_f = 0.4 (30% ethyl acetate/hexane); ^{1}H NMR (300 MHz, CDCl$_3$); δ 3.89

10172 | Org. Biomol. Chem., 2015, **13**, 10162–10178

This journal is © The Royal Society of Chemistry 2015

(s, 3H, –OCH$_3$), 3.90 (s, 3H, –OCH$_3$), 6.90 (s, 1H, ArH), 7.26–7.49 (m, 2H, ArH), 7.88–7.97 (m, 1H, ArH) 10.18 (s, 1H, –CHO) ppm; MS (ESI) m/z 234 [M + H].

3-(4-Methoxyphenyl)isoxazole-5-carbaldehyde 18c. This compound was prepared by the addition of (3-(4-methoxyphenyl)isoxazol-5-yl)methanol **17c** (2.05 g. 10 mmol) and IBX (3.36 g 1.2 mmol). Yellow solid (1.72 g, yield 85%): R_f = 0.5 (25% ethyl acetate/hexane); ^{1}H NMR (500 MHz, CDCl$_3$); δ 3.87 (s, 3H, –OCH$_3$), 6.79 (s, 1H, ArH), 7.02 (d, 2H, J = 8.8 Hz, ArH), 7.77 (d, 2H, J = 9.0 Hz, ArH), 10.19 (s, 1H, –CHO) ppm; MS (ESI) m/z 204 [M + H].

3-(Benzo[*d*][1,3]dioxol-5-yl)isoxazole-5-carbaldehyde 18d. This compound was prepared by the addition of (3-(benzo[*d*]-[1,3]dioxol-5-yl)isoxazol-5-yl)methanol **17d** (2.19 g 10 mmol) and IBX (3.36 g 1.2 mmol). Yellow solid (1.8 g, yield 83%): R_f = 0.6 (30% ethyl acetate/hexane); ^{1}H NMR (300 MHz, CDCl$_3$); δ 6.06 (s, 2H, –OCH$_2$O), 6.75 (s, 1H, ArH), 6.92 (d, 1H, J = 8.2 Hz, ArH), 7.29 (s, 1H, ArH), 7.36 (d, 1H, J = 8.0 Hz, ArH), 10.16 (s, 1H, –CHO) ppm; MS (ESI) m/z 218 [M + H].

Preparation of (*E*)-ethyl 3-(3-arylisoxazol-5-yl)acrylate 19a–d

To each of the isoxazole carbaldehydes obtained in the above step was added an equimolar amount of (carbethoxymethylene)triphenylphosphine (Ph$_3$PCHCO$_2$C$_2$H$_5$, C2-wittig reagent) in toluene at room temperature and continued stirring for 3–4 h. After performing TLC toluene was evaporated and appropriate amounts of water were added. The crude compounds were extracted by ethyle acetate (50 ml × 4). The organic layer was dried on anhydrous Na$_2$SO$_4$ and ethyl acetate was evaporated to obtain crude α,β-unsaturated isoxazole esters **19a–d** in good yields (70–75%).

(*E*)-Ethyl 3-(3-(3,4,5-trimethoxyphenyl)isoxazol-5-yl)acrylate 19a. This compound was prepared by the addition of 3-(3,4,5-trimethoxyphenyl)isoxazole-5-carbaldehyde **18a** (263 mg 1.0 mmol) and Ph$_3$PCHCO$_2$C$_2$H$_5$ (248 mg 1.0 mmol). Pale yellow solid (233 mg, yield 70%): R_f = 0.5 (30% ethyl acetate/hexane); ^{1}H NMR (300 MHz, CDCl$_3$); δ 1.36 (t, 3H, J = 7.1 Hz, –CH$_3$), 3.91 (s, 3H, –OCH$_3$), 3.94 (s, 6H, –OCH$_3$), 4.30 (q, 2H, J_1 = 7.1 Hz, J_2 = 6.9 Hz, –CH$_2$), 6.57 (d, 1H, *trans*H J = 16.0 Hz), 6.65 (s, 1H, ArH), 7.02 (s, 2H, ArH), 7.70 (d, 1H, *trans*H J = 16.2 Hz) ppm; ^{13}C NMR (75 MHz, CDCl$_3$): 12.5, 54.6, 58.8, 59.1, 96.2, 101.6, 104.1, 107.9, 120.5, 124.4, 129.7, 138.0, 151.8, 158.7, 163.2, 163.6, 168.5 ppm; MS (ESI) m/z 334 [M + H]; HR-MS (ESI) m/z for C$_{17}$H$_{20}$O$_6$N calculated m/z: 334.1212, found m/z: 334.1206.

(*E*)-Ethyl 3-(3-(3,4-dimethoxyphenyl)isoxazol-5-yl)acrylate 19b. This compound was prepared by the addition of 3-(3,4-dimethoxyphenyl)isoxazole-5-carbaldehyde **18b** (233 mg 1.0 mmol) and Ph$_3$PCHCO$_2$C$_2$H$_5$ (248 mg 1.0 mmol). Yellow solid (218 mg, yield 72%): R_f = 0.5 (30% ethyl acetate/hexane); ^{1}H NMR (300 MHz, CDCl$_3$); δ 1.35 (t, 3H, J = 7.1 Hz, –CH$_3$), 3.93 (s, 3H, –OCH$_3$), 3.94 (s, 3H, –OCH$_3$), 4.15–4.31 (q, 2H, J_1 = 7.0 Hz, J_2 = 7.1 Hz, –CH$_2$), 6.23 (s, 1H, ArH), 6.62 (s, 1H, ArH), 6.72 (d, 1H, *trans*H J = 16.2 Hz), 6.92 (d, 1H, J = 8.4 Hz, ArH), 6.42 (d, 1H, *trans*H J = 16.2 Hz), 7.20–7.28 (m, 1H, ArH) ppm; ^{13}C NMR (75 MHz, CDCl$_3$): 12.5, 54.2, 54.2, 59.1, 95.1, 107.3,

110.1, 117.4, 117.8, 124.2, 129.8, 147.5, 149.2, 158.6, 163.6, 168.6 ppm; MS (ESI) m/z 304 [M + H]; HR-MS (ESI) m/z for C$_{16}$H$_{18}$O$_5$N calculated m/z: 304.1106, found m/z: 304.1109.

(*E*)-Ethyl 3-(3-(4-methoxyphenyl)isoxazol-5-yl)acrylate 19c. This compound was prepared by the addition of 3-(3-(4-methoxyphenyl)isoxazole-5-carbaldehyde **18c** (203 mg 1.0 mmol) and Ph$_3$PCHCO$_2$C$_2$H$_5$ (248 mg 1.0 mmol). Yellow solid (204.7 mg, yield 75%): R_f = 0.4 (30% ethyl acetate/hexane); ^{1}H NMR (300 MHz, CDCl$_3$); δ 1.35 (t, 3H, J = 7.1 Hz, –CH$_3$), 3.87 (s, 3H, –OCH$_3$), 4.23–4.34 (q, 2H, J_1 = 7.0 J_2 = 7.1 Hz, –CH$_2$), 6.54 (d, 1H, *trans*H J = 16.1 Hz), 6.58 (s, 1H, ArH), 6.99 (d, 2H, J = 8.3 Hz, ArH), 7.68 (d, 1H, *trans*H J = 16.1 Hz), 7.73 (d, 2H, J = 8.8 Hz, ArH) ppm; ^{13}C NMR (75 MHz, CDCl$_3$): 14.1, 55.3, 60.9, 95.4, 114.4, 119.6, 125.3, 129.1, 127.4, 127.9, 131.8, 160.1, 161.3, 165.6, 170.6 ppm; MS (ESI) m/z 274 [M + H]; HR-MS (ESI) m/z for C$_{15}$H$_{16}$O$_4$N calculated m/z: 274.1001, found m/z: 274.1002.

(*E*)-Ethyl 3-(3-(benzo[*d*][1,3]dioxol-5-yl)isoxazol-5-yl)acrylate 19d. This compound was prepared by the addition of 3-(benzo-[*d*][1,3]dioxol-5-yl)isoxazole-5-carbaldehyde **18d** (217 mg 1.0 mmol) and Ph$_3$PCHCO$_2$C$_2$H$_5$ (248 mg 1.0 mmol). Yellow solid (212 mg, yield 75%): R_f = 0.5 (30% ethyl acetate/hexane); ^{1}H NMR (300 MHz, CDCl$_3$); δ 1.23 (t, 3H, J = 7.0 Hz, –CH$_3$), 4.15–4.33 (q, 2H, J = 6.0 Hz, –CH$_2$), 6.01 (s, 2H, –OCH$_2$O–), 6.45 (s, 1H, ArH), 6.67 (d, 1H, *trans*H J = 16.0 Hz), 6.72–6.78 (m, 1H, ArH), 6.92 (s, 1H, ArH), 7.11–7.35 (m, 1H, ArH), 7.63 (d, 1H, *trans*H J = 15.9 Hz) ppm; ^{13}C NMR (75 MHz, CDCl$_3$): 14.1, 56.2, 61.0, 96.6, 103.1, 122.1, 125.6, 131.6, 140.1, 153.6, 160.2, 165.5, 170.5 ppm; MS (ESI) m/z 288 [M + H]; HR-MS (ESI) m/z for C$_{15}$H$_{17}$O$_3$N$_2$ calculated m/z: 288.0793, found m/z: 288.0796.

Preparation of (*E*)-3-(3-arylisoxazol-5-yl)acrylic acids 20a–d

To each of the (*E*)-ethyl 3-(3-arylisoxazol-5-yl)acrylates **19a–d** obtained in the above step was added equimolar amounts of lithium hydroxide (LiOH·H$_2$O) in a mixture of solvents THF : MeOH : H$_2$O (3 : 1 : 1) at room temperature and continued stirring for 3–4 h. After performing TLC the solvent mixture was evaporated and appropriate amounts of water were added. The crude compounds were extracted by ethyle acetate (50 ml × 4). The aqueous layer was acidified using dil. HCl, and then again extracted by ethyl acetate (50 ml × 4). The organic layer was dried on anhydrous Na$_2$SO$_4$ and ethyl acetate was evaporated to obtain the corresponding pure α,β-unsaturated isoxazole acids **20a–d** in good yields (80–85%).

General procedure for the synthesis of isoxazole linked arylcinnamides 21a–n

To the (*E*)-3-(3-arylisoxazol-5-yl)acrylic acid **20a–d** prepared in the above step was added an equimolar amount of EDCI and catalytic amount of hydroxybenzotriazole (Hobt) in ice cold dichloromethane. After 10 min appropriate amounts of aryl amines were added at 0 °C and stirring was continued at room temperature for 8 h. The progress of the reaction was monitored by TLC. After completion of the reaction an appropriate amount of sodium bicarbonate (NaHCO$_3$) solution was added and subsequently the final compounds were extracted with

ethyl acetate (50 ml × 4). The organic layers so obtained were washed with 5% HCl solution and the organic solvent was evaporated to afford crude compounds. Further these compounds were purified using column chromatography by using ethyl acetate and a hexane solvent system to get pure compounds in good yields (65–78%).

(E)-N-(3,4,5-Trimethoxyphenyl)-3-(3-(3,4,5-trimethoxyphenyl)-isoxazol-5-yl)acrylamide 21a. This compound was prepared by the addition of (E)-3-(3-(3,4,5-trimethoxyphenyl)isoxazol-5-yl)-acrylic acid **20a** (305 mg 1.0 mmol) and 3,4,5-trimethoxyaniline **14a** (183 mg 1.0 mmol). Pale yellow solid, yield: 340 mg (75%); mp: 202–204 °C; ^{1}H NMR (300 MHz, CDCl$_3$ + DMSO-d$_6$); δ 3.84 (s, 3H, –OCH$_3$), 3.87 (s, 6H, –OCH$_3$), 3.91 (s, 3H, –OCH$_3$), 3.94 (s, 6H, –OCH$_3$), 6.61 (s, 1H, ArH), 6.78 (d, 1H, transH J = 15.8 Hz), 6.96 (s, 1H, J = 7.5 Hz, ArH) 7.00 (s, 2H, J = 8.8 Hz, ArH) 7.69 (d, 1H, transH, J = 15.4 Hz), 7.67(s, 1H, ArH); ^{13}C NMR (75 MHz, CDCl$_3$ + DMSO-d$_6$): δ 54.4, 54.8, 59.0, 96.0, 96.4, 101.8, 120.8, 125.4, 128.2, 132.7, 133.6, 138.3, 151.4, 152.1, 159.1, 161.2, 168.6 ppm; IR (KBr) (ν_{max}/cm^{-1}): ν = 3315, 2997, 1680, 1549, 1520, 1484, 1454, 1420, 1376, 1312, 1273, 1204, 1181, 1142, 1026 cm^{-1}; MS (ESI) m/z 471; HR-MS (ESI) m/z for C$_{24}$H$_{27}$O$_8$N$_2$ calculated m/z: 471.1742, found m/z: 471.1761.

(E)-N-(3,4-Dimethoxyphenyl)-3-(3-(3,4,5-trimethoxyphenyl)-isoxazol-5-yl)acrylamide 21b. This compound was prepared by the addition of **20a** (150 mg 1.0 mmol) and 3,4-dimethoxy-aniline **14b** (153 mg 1.0 mmol). Colourless solid, yield: 295 mg (67%); mp: 182–184 °C; ^{1}H NMR (500 MHz, CDCl$_3$ + DMSO-d$_6$); δ 3.80 (s, 6H, –OCH$_3$), 3.89 (s, 3H, –OCH$_3$), 3.95 (s, 6H, –OCH$_3$), 6.23 (s, 1H, ArH), 6.78 (s, 1H, ArH), 6.97 (d, 1H, transH J = 15.6 Hz), 7.02 (s, 1H, ArH), 7.05 (s, 2H, ArH), 7.54 (s, 1H, ArH), 7.62 (d, 1H, transH J = 15.6 Hz) 9.92 (brs, 1H, –NH); IR (KBr) (ν_{max}/cm^{-1}): ν = 3314, 2937, 1686, 1611, 1507, 1458, 1425, 1412, 1242, 1131, 999 cm^{-1}; MS (ESI) m/z 441 [M + H]; HR-MS (ESI) m/z for C$_{23}$H$_{25}$O$_7$N$_2$ calculated m/z: 441.1656, found m/z: 441.1641.

(E)-N-(4-Methoxyphenyl)-3-(3-(3,4,5-trimethoxyphenyl)isoxazol-5-yl)acrylamide 21c. This compound was prepared by the addition of **20a** (150 mg 1.0 mmol) and 4-methoxyaniline **14c** (123 mg 1.0 mmol). Pale yellow solid, yield: 300 mg (73%); mp: 186–188 °C; ^{1}H NMR (300 MHz, DMSO-d$_6$); δ 3.79 (s, 3H, –OCH$_3$), 3.87 (s, 3H, –OCH$_3$), 3.95 (s, 6H, –OCH$_3$), 6.87 (d, 2H, J = 8.4 Hz, ArH), 6.99 (d, 1H, transH J = 15.6 Hz), 7.08 (s, 2H, ArH), 7.53–7.74 (m, 3H, ArH), 7.66 (d, 1H, transH J = 15.6 Hz), 10.03 (brs, 1H, –NH); ^{13}C NMR (75 MHz, DMSO-d$_6$): δ 53.7, 54.7, 58.9, 96.4, 101.7, 112.3, 119.7, 120.7, 125.4, 128.3, 130.5, 138.1, 151.9, 154.3, 159.0, 160.8, 168.4 ppm; IR (KBr) (ν_{max}/cm^{-1}): ν = 3286, 3040, 1680, 1630, 1573, 1544, 1512, 1475, 1426, 1390, 1315, 1227, 1210, 1184, 1112, 1036, 990 cm^{-1}; MS (ESI) m/z 411 [M + H]; HR-MS (ESI) m/z for C$_{22}$H$_{23}$O$_6$N$_2$ calculated m/z: 411.1550, found m/z: 411.1542.

(E)-N-(3,4-Difluorophenyl)-3-(3-(3,4,5-trimethoxyphenyl)-isoxazol-5-yl)acrylamide 21d. This compound was prepared by the addition of **20a** (305 mg 1.0 mmol) and 3,4-difluoro-aniline **14d** (130 mg 1.0 mmol). Brown solid, yield: 290 mg (70%);

mp: 192–194 °C; ^{1}H NMR (500 MHz, CDCl$_3$ + DMSO-d$_6$); δ 3.84 (s, 3H, –OCH$_3$), 3.96 (s, 6H, –OCH$_3$), 6.91–7.05 (m, 2H, ArH), 7.06–7.23 (m, 2H, ArH), 7.37 (s, 2H, ArH), 7.61 (d, 1H, transH J = 16.0 Hz), 7.88 (d, 1H, transH J = 16.4 Hz, ArH) 10.40 (brs, 1H, –NH); ^{13}C NMR (75 MHz, CDCl$_3$ + DMSO-d$_6$): δ 55.0, 59.4, 96.6, 102.0, 107.7, 108.0, 114.4, 115.6, 115.9, 121.0, 126.7, 127.9, 152.3, 159.2, 161.7, 168.8 ppm; IR (KBr) (ν_{max}/cm^{-1}): ν = 3309, 2940, 1669, 1624, 1574, 1518, 1505, 1424, 1241, 967 cm^{-1}; MS (ESI) m/z 417 [M + H]; HR-MS (ESI) m/z for C$_{21}$H$_{19}$F$_2$O$_5$N$_2$ calculated m/z: 417.1256, found m/z: 417.1247.

(E)-3-(3-(3,4-Dimethoxyphenyl)isoxazol-5-yl)-N-(3,4,5-trimethoxyphenyl)acrylamide 21e. This compound was prepared by the addition of (E)-3-(3-(3,4-dimethoxyphenyl)isoxazol-5-yl)-acrylic acid **20b** (275 mg 1.0 mmol) and 3,4,5-trimethoxyaniline **14a** (183 mg 1.0 mmol). Yellow solid, yield: 300 mg (68%); mp: 212–214 °C; ^{1}H NMR (300 MHz, CDCl$_3$ + DMSO-d$_6$); δ 3.69 (s, 3H, –OCH$_3$), 3.80 (s, 6H, –OCH$_3$), 3.87 (s, 3H, –OCH$_3$), 3.91 (s, 3H, –OCH$_3$), 7.00 (d, 1H, transH J = 15.6 Hz), 7.07 (s, 1H, ArH), 7.13 (s, 1H, ArH), 7.31 (d, 1H, transH J = 14.9 Hz), 7.34–7.44 (m, 1H, ArH), 7.45–7.51 (m, 1H, ArH), 7.52–7.60 (m, 1H, ArH), 7.84 (d, 1H, ArH J = 8.3 Hz), 10.43 (brs, 1H, –NH); ^{13}C NMR (75 MHz, CDCl$_3$ + DMSO-d$_6$): δ 55.5, 60.1, 96.4, 97.1, 108.5, 109.7, 111.2, 118.2, 118.7, 119.3, 123.6, 125.4, 127.1, 133.7, 134.7, 148.8, 152.5, 160.1, 162.4, 169.7 ppm; IR (KBr) (ν_{max}/cm^{-1}): ν = 3320, 2940, 1687, 1610, 1596, 1502, 1465, 1427, 1416, 1283, 1133, 1019, 996 cm^{-1}; MS (ESI) m/z 441 [M + H]; HR-MS (ESI) m/z for C$_{23}$H$_{25}$O$_7$N$_2$ calculated m/z: 441.1656, found m/z: 441.1644.

(E)-N-(3,4-Dimethoxyphenyl)-3-(3-(3,4-dimethoxyphenyl)-isoxazol-5-yl)acrylamide 21f. This compound was prepared by the addition of **20b** (275 mg 1.0 mmol) and 3,4-dimethoxy-aniline **14b** (153 mg 1.0 mmol). The compound obtained as yellow crystals, yield: 305 mg (74%); mp: 196–198 °C; ^{1}H NMR (400 MHz, CDCl$_3$ + DMSO-d$_6$); δ 3.79 (s, 6H, –OCH$_3$), 3.94 (s, 3H, –OCH$_3$), 3.97 (s, 3H, –OCH$_3$), 6.22 (s, 1H, ArH), 6.80–6.90 (m, 1H, ArH), 6.96 (s, 1H, ArH), 6.99–7.04 (m, 3H, ArH), 7.33 (d, 1H, transH J = 15.1 Hz), 7.42 (d, 1H, ArH J = 9.8 Hz), 7.61 (d, 1H, transH J = 15.6 Hz), 7.66–7.71 (m, 1H, ArH), 10.71 (brs, 1H, –NH); IR (KBr) (ν_{max}/cm^{-1}): ν = 3330, 3010, 2910, 1671, 1620, 1566, 1511, 1469, 1443, 1383, 1221, 1116, 1026, 989 cm^{-1}; MS (ESI) m/z 411 [M + H]; HR-MS (ESI) m/z for C$_{22}$H$_{23}$O$_6$N$_2$ calculated m/z: 411.1550, found m/z: 411.1547.

(E)-3-(3-(3,4-Dimethoxyphenyl)isoxazol-5-yl)-N-(4-methoxy-phenyl)acrylamide 21g. This compound was prepared by the addition of **20b** (275 mg 1.0 mmol) and 4-methoxyaniline **14c** (123 mg 1.0 mmol). Brown solid, yield: 290 mg (76%); mp: 208–210 °C; ^{1}H NMR (300 MHz, CDCl$_3$ + DMSO-d$_6$); δ 3.79 (s, 3H, –OCH$_3$), 3.91 (s, 3H, –OCH$_3$), 3.94 (s, 3H, –OCH$_3$), 6.86 (d, 2H, ArH J = 8.6 Hz), 6.97–7.04 (m, 1H, ArH), 7.37 (s, 1H, ArH), 7.45 (d, 1H, ArH J = 8.3 Hz), 7.55 (d, 1H, transH J = 15.6 Hz), 7.65 (d, 2H, J = 8.8 Hz ArH), 7.92 (d, 1H, transH J = 15.6 Hz), H J = 9.8 Hz), 7.91 (s, 1H, –ArH), 10.17 (brs, 1H, –NH); ^{13}C NMR (75 MHz, CDCl$_3$ + DMSO-d$_6$): δ 54.9, 55.4, 96.7, 108.7, 111.6, 113.6, 118.7, 119.2, 120.8, 126.5, 129.6, 148.9, 150.5,

10174 | Org. Biomol. Chem., 2015, 13, 10162–10178

This journal is © The Royal Society of Chemistry 2015

155.4, 160.2, 161.9, 169.7 ppm; IR (KBr) (ν_{max}/cm^{-1}): ν = 3290, 3033, 3010, 1682, 1615, 1574, 1526, 1419, 1376, 1320, 1026, 993 cm^{-1}; MS (ESI) m/z 381 [M + H]. HR-MS (ESI) m/z for $C_{21}H_{21}O_5N_2$ calculated m/z: 381.1445, found m/z: 381.1454.

(E)-N-(3,4-Difluorophenyl)-3-(3-(3,4-dimethoxyphenyl)isoxazol-5-yl)acrylamide 21h. This compound was prepared by the addition of **20b** (275 mg 1.0 mmol) and 3,4-difluoroaniline **14d** (130 mg 1.0 mmol). Yellow solid, yield: 295 mg (75%); mp: 216–218 °C; ^{1}H NMR (400 MHz, CDCl$_3$ + DMSO-d$_6$); δ 3.91 (s, 3H, –OCH$_3$), 3.96 (s, 3H, –OCH$_3$), 6.75 (d, 1H, transH, J = 15.6 Hz), 6.93 (d, 1H, ArH, J = 8.3 Hz), 7.05–7.22 (m, 1H, ArH), 7.29–7.41 (m, 2H, ArH), 7.55 (s, 2H, ArH), 7.65 (d, 1H, transH, J = 15.8 Hz), 7.81–7.93 (m, 1H, ArH), 10.05 (brs, 1H, –NH); ^{13}C NMR (75 MHz, CDCl$_3$ + DMSO-d$_6$): δ ppm; IR (KBr) (ν_{max}/cm^{-1}): ν = 3230, 3010, 1640, 1610, 1586, 1550, 1496, 1480, 1410, 1380, 1254, 1200, 1175, 1110, 1026, 993 cm^{-1}; MS (ESI) m/z 387 [M + H]; HR-MS (ESI) m/z for $C_{20}H_{17}F_2O_4N_2$ calculated m/z: 387.1150, found m/z: 387.1147.

(E)-3-(3-(4-Methoxyphenyl)isoxazol-5-yl)-N-(3,4,5-trimethoxyphenyl)acrylamide 21i. This compound was prepared by the addition of (E)-3-(3-(4-methoxyphenyl)isoxazol-5-yl)acrylic acid **20c** (245 mg 1.0 mmol) and 3,4,5-trimethoxyaniline **14a** (183 mg 1.0 mmol). Pale yellow solid yield: 305 mg (74%); mp: 168–170 °C; ^{1}H NMR (500 MHz, CDCl$_3$ + DMSO-d$_6$); δ 3.84 (s, 3H, –OCH$_3$), 3.88 (s, 9H, –OCH$_3$), 6.55 (s, 1H, ArH), 6.73 (d, 1H, J = 16.1 Hz, transH), 6.93 (s, 1H, ArH), 7.00 (d, 2H, J = 8.3 Hz, ArH), 7.41 (s, 1H, ArH), 7.69 (d, 1H, J = 16.1 Hz, transH), 7.73 (d, 2H, J = 9.0 Hz, ArH); ^{13}C NMR (75 MHz, CDCl$_3$ + DMSO-d$_6$): δ 55.0, 55.5, 60.0, 96.1, 97.1, 114.2, 119.1, 127.0, 129.2, 133.7, 134.7, 152.5, 160.1, 162.3, 169.7 ppm; IR (KBr) (ν_{max}/cm^{-1}): ν = 3292, 3060, 1685, 1650, 1584, 1524, 1473, 1444, 1363, 1315, 1296, 1145, 1064, 996 cm^{-1}; MS (ESI) m/z 411 [M + H]; HR-MS (ESI) m/z for $C_{22}H_{23}O_6N_2$ calculated m/z: 411.0953, found m/z: 411.0950.

(E)-N-(3,4-Dimethoxyphenyl)-3-(3-(4-methoxyphenyl)isoxazol-5-yl)acrylamide 21j. This compound was prepared by the addition of **20c** (245 mg 1.0 mmol) and 3,4-dimethoxyaniline **14b** (153 mg 1.0 mmol). Yellow solid, yield: 296 mg (78%); mp: 196–198 °C; ^{1}H NMR (500 MHz, CDCl$_3$ + DMSO-d$_6$); δ 3.78 (s, 6H, –OCH$_3$), 3.87 (s, 3H, –OCH$_3$), 6.21 (s, 1H, ArH), 6.90–7.09 (m, 4H, ArH), 6.64 (d, 1H, J = 16.0 Hz, transH), 7.46–7.58 (m, 1H, ArH), 7.66 (d, 1H, J = 16.0 Hz, transH), 7.74–7.82 (m, 1H, ArH), 7.86–7.99 (m, 1H, ArH), 10.27 (brs, 1H, –NH); ^{13}C NMR (75 MHz, CDCl$_3$ + DMSO-d$_6$): δ 54.7, 54.9, 95.7, 95.8, 96.0, 97.7, 109.3, 114.1, 118.4, 119.1, 124.1, 126.5, 126.4, 127.0, 127.3, 130.7, 140.1, 159.9, 160.3, 160.8, 162.5, 166.5, 169.7 ppm; IR (KBr) (ν_{max}/cm^{-1}): ν = 3290, 3033, 3010, 1682, 1615, 1574, 1526, 1419, 1376, 1320, 1026, 993 cm^{-1}; MS (ESI) m/z 381 [M + H]; HR-MS (ESI) m/z for $C_{21}H_{21}O_5N_2$ calculated m/z: 381.1445, found m/z: 381.1454.

(E)-N-(3,4-Difluorophenyl)-3-(3-(4-methoxyphenyl)isoxazol-5-yl)acrylamide 21k. This compound was prepared by the addition of **20c** (245 mg 1.0 mmol) and 3,4-difluoroaniline **14d** (130 mg 1.0 mmol). Pale yellow solid, yield: 265 mg (74%); mp: 186–188 °C; ^{1}H NMR (300 MHz, CDCl$_3$ + DMSO-d$_6$); δ 3.88 (s, 3H, –OCH$_3$), 6.84 (s, 1H, ArH), 6.98 (d, 1H, transH J = 15.6 Hz), 7.02 (d, 2H, J = 9.0 Hz, ArH), 7.07–7.23 (m, 1H, ArH), 7.39 (d, 1H, J = 8.4 Hz, ArH), 7.61 (d, 1H, J = 15.6 Hz, transH), 7.77 (d, 2H, J = 8.4 Hz, ArH), 7.82–7.97 (m, 1H, ArH), 10.47 (brs, 1H, –NH); ^{13}C NMR (75 MHz, CDCl$_3$ + DMSO-d$_6$): δ 55.1, 96.3, 108.4, 108.6, 114.3, 115.4, 116.8, 117.0, 119.1, 127.1, 127.7, 128.8, 135.6, 160.1, 160.8, 162.5, 169.8 ppm; IR (KBr) (ν_{max}/cm^{-1}): ν = 3233, 3060, 2961, 1663, 1620, 1543, 1518, 1437, 1305, 1253, 1214, 1175, 1030, 968 cm^{-1}; MS (ESI) m/z 357 [M + H]; HR-MS (ESI) m/z for $C_{19}H_{15}O_3F_2N_2$ calculated m/z: 357.1045, found m/z: 357.1041.

(E)-3-(3-(Benzo[d][1,3]dioxol-5-yl)isoxazol-5-yl)-N-(3,4,5-trimethoxyphenyl)acrylamide 21l. This compound was prepared by the addition of (E)-3-(3-(benzo[d][1,3]dioxol-5-yl)isoxazol-5-yl)acrylic acid **20d** (258 mg 1.0 mmol) and 3,4,5-trimethoxyaniline (183 mg 1.0 mmol) (**14a**). The compound was obtained as a yellow solid, yield: 315 mg (74%); mp: 165–167 °C; ^{1}H NMR (400 MHz, CDCl$_3$ + DMSO-d$_6$); δ 3.80 (s, 3H, –OCH$_3$), 3.89 (s, 6H, –OCH$_3$), 6.07 (s, 2H, –OCH$_2$O–), 6.75 (s, 1H, ArH), 6.86–6.97 (m, 1H, ArH), 7.04 (d, 1H, J = 16.0 Hz, transH), 7.13 (s, 1H, ArH), 7.30–7.47 (m, 2H, ArH), 7.62 (d, 1H, J = 15.8 Hz, transH), 7.88 (d, 1H, J = 8.1 Hz, ArH), 10.05 (brs, 1H, –NH); IR (KBr) (ν_{max}/cm^{-1}): ν = 3339, 3128, 2937, 1667, 1636, 1599, 1490, 1505, 1431, 1410, 1233, 1127, 1039, 806 cm^{-1}; MS (ESI) m/z 425 [M + H]; HR-MS (ESI) m/z for $C_{22}H_{21}O_7N_2$ calculated m/z: 425.1343, found m/z: 425.1350.

(E)-3-(3-(Benzo[d][1,3]dioxol-5-yl)isoxazol-5-yl)-N-(3,4-dimethoxyphenyl)acrylamide 21m. This compound was prepared by the addition of **20d** (258 mg 1.0 mmol) and 3,4-dimethoxyaniline **14b** (153 mg 1.0 mmol). Brown solid, yield: 287 mg (73%); mp: 182–184 °C; ^{1}H NMR (500 MHz, CDCl$_3$ + DMSO-d$_6$); δ 3.77 (s, 6H, –OCH$_3$), 6.07 (s, 2H, –OCH$_2$O–), 6.73–7.02 (m, 4H, ArH), 7.25–7.42 (m, 2H, ArH), 7.34 (d, 1H, transH J = 14.8 Hz), 7.55 (d, 1H, transH J = 15.8 Hz), 7.76–7.91 (m, 1H, ArH), 10.1 (brs, 1H, –NH); ^{13}C NMR (75 MHz, CDCl$_3$ + DMSO-d$_6$): δ 53.4, 94.2, 95.3, 96.3, 100.0, 104.1, 107.1, 118.6, 119.0, 125.7, 127.9, 138.8, 146.4, 147.6, 158.7, 158.9, 158.8, 159.4, 160.9, 168.0 ppm; IR (KBr) (ν_{max}/cm^{-1}): ν = 3326, 3112, 2940, 1670, 1646, 1587, 1541, 1467, 1414, 1309, 1284, 1256, 1145, 1048, 908 cm^{-1}; MS (ESI) m/z 395 [M + H]; HR-MS (ESI) m/z for $C_{21}H_{19}O_6N_2$ calculated m/z: 395.1246, found m/z: 395.1245.

(E)-3-(3-(Benzo[d][1,3]dioxol-5-yl)isoxazol-5-yl)-N-(3,4-difluorophenyl)acrylamide 21n. This compound was prepared by the addition of **20d** (258 mg 1.0 mmol) and 3,4-difluoroaniline **14d** (130 mg 1.0 mmol). Pale yellow solid, yield: 275 mg (75%); mp: 196–198 °C; ^{1}H NMR (300 MHz, CDCl$_3$ + DMSO-d$_6$); δ 6.08 (s, 2H, –OCH$_2$O–), 6.75 (s, 4H, ArH), 7.93 (d, 1H, J = 15.8 Hz, transH), 6.94 (s, 1H, ArH), 7.05–7.20 (m, 1H, ArH), 7.32–7.45 (m, 2H, ArH), 7.61 (d, 1H, J = 15.6 Hz, transH), 7.64 (s, 1H, ArH), 7.81–7.94 (m, 1H, ArH), 10.1 (brs, 1H, –NH); ^{13}C NMR (75 MHz, CDCl$_3$ + DMSO-d$_6$): δ 95.3, 100.0, 104.1, 107.1, 113.9, 117.0, 118.7, 119.0, 126.1, 127.4, 134.0, 146.4, 147.6, 158.6, 161.0, 168.1 ppm; IR (KBr) (ν_{max}/cm^{-1}): ν = 3315, 3097, 3014, 1680, 1656, 1593, 1533, 1476, 1440, 1339, 1308, 1274, 1215, 1145, 1026, 924 cm^{-1}; MS (ESI) m/z 371 [M + H]; HR-MS (ESI) m/z for $C_{19}H_{13}O_4F_2N_2$ calculated m/z: 371.0837, found m/z: 371.0846.

Biology

Cell cultures, maintenance and antiproliferative evaluation. Cell lines used in this study were purchased from the American Type Culture Collection (ATCC, United States). A549, MDA-MB231, and HeLa cells were grown in Dulbecco's modified Eagle's medium (containing 10% FBS under a humidified atmosphere of 5% CO_2 at 37 °C). DU145 cells were cultured in Eagle's minimal essential medium (MEM) containing non-essential amino acids, 1 mM sodium pyruvate, 10 mg per mL bovine insulin, and 10% FBS. Cells were trypsinized when sub-confluent from T25 flasks/60 mm dishes and seeded in 96-well plates. The synthesized test compounds were evaluated for their *in vitro* antiproliferative effects in four different human cancer cell lines. A protocol of 48 h continuous drug exposure was used, and an MTT cell proliferation assay was used to estimate cell viability or growth. The cell lines were grown in their respective media containing 10% fetal bovine serum and were seeded into 96-well microtiter plates in 200 μL aliquots at plating densities depending on the doubling time of individual cell lines. The microtiter plates were incubated at 37 °C, 5% CO_2, 95% air, and 100% relative humidity for 24 h prior to the addition of experimental drugs. Aliquots of 2 μL of the test compounds were added to the wells already containing 198 μL of cells, resulting in the required final drug concentration. For each compound, four concentrations (1, 10, 100, and 1000 μM) were evaluated, and each evaluation was done in triplicate wells. Plates were incubated further for 48 h, and the assay was terminated by the addition of 10 μL of 5% MTT and incubated for 60 min at 37 °C. Later, the plates were air-dried. The bound stain was subsequently eluted with 100 μL of DMSO, and the absorbance was read on a multimode plate reader (Tecan M200) at a wavelength of 560 nm. Percent growth was calculated on a plate by plate basis for test wells relative to control wells. The above procedure was repeated thrice. The growth inhibitory effects of the compounds were analyzed by generating dose response curves as a plot of the percentage surviving cells *versus* compound concentration. The sensitivity of the cancer cells to the test compound was expressed in terms of IC_{50}, a value defined as the concentration of a compound that produced 50% reduction as compared to the control absorbance. IC_{50} values are indicated as mean ± SD of the three independent experiments.[15]

Analysis of cell cycle. HeLa cells in 60 mm dishes were incubated for 24 h in the presence or absence of test compounds **15a**, **15b** and **15e** at 2 μM concentration. Cells were harvested with Trypsin-EDTA, fixed with ice-cold 70% ethanol at 4 °C for 30 min, ethanol was removed by centrifugation and cells were stained with 1 mL of DNA staining solution [0.2 mg of Propidium Iodide (PI) and 2 mg RNase A] for 30 min as described earlier. The DNA contents of 20 000 events were measured by a flow cytometer (BD FACSCanto II). Histograms were analyzed using FCS express 4 plus.[15]

Tubulin polymerization assay. An *in vitro* assay for monitoring the time-dependent polymerization of tubulin to microtubules was performed employing a fluorescence-based tubulin polymerization assay kit (BK011, Cytoskeleton, Inc.) according to the manufacturer's protocol. The reaction mixture in a final volume of 10 μl in PEM buffer (80 mM PIPES, 0.5 mM EGTA, 2 mM $MgCl_2$, pH 6.9) in 384 well plates contained 2 mg per mL of bovine brain tubulin, 10 μM fluorescent reporter, 1 mM GTP in the presence or absence of test compounds at 37 °C. Tubulin polymerization was followed by monitoring the fluorescence enhancement due to the incorporation of a fluorescence reporter into microtubules as polymerization proceeds. Fluorescence emission at 420 nm (excitation wavelength is 360 nm) was measured for 1 h at 1 min intervals in a multimode plate reader (Tecan M200). To determine the IC_{50} values of the compounds against tubulin polymerization, the compounds were pre-incubated with tubulin at varying concentrations (1, 5, 10 and 20 μM). Assays were performed under similar conditions to those employed for polymerization assays as described above.[15]

Western blot analysis of soluble *versus* polymerized tubulin and cyclin B1. Cells were seeded in 12-well plates at 1×10^5 cells per well in complete growth medium. Following treatment of cells with respective compounds (**15a**, **15b** and **15e**) for a duration of 24 h, cells were washed with PBS and subsequently soluble and insoluble tubulin fractions were collected. To collect the soluble tubulin fractions, cells were permeabilized with 200 μL of pre-warmed lysis buffer [80 mM Pipes-KOH (pH 6.8), 1 mM $MgCl_2$, 1 mM EGTA, 0.2% Triton X-100, 10% glycerol, 0.1% protease inhibitor cocktail (Sigma-Aldrich)] and incubated for 3 min at 30 °C. Lysis buffer was gently removed, and mixed with 100 μL of 3 × Laemmli's sample buffer (180 mM Tris-Cl pH 6.8, 6% SDS, 15% glycerol, 7.5% β-mercaptoethanol and 0.01% bromophenol blue). Samples were immediately heated to 95 °C for 3 min. To collect the insoluble tubulin fraction, 300 μL of 1 × Laemmli's sample buffer was added to the remaining cells in each well, and the samples were heated to 95 °C for 3 min. Equal volumes of samples were run on an SDS-10% polyacrylamide gel and were transferred to a nitrocellulose membrane employing semidry transfer at 50 mA for 1 h. Blots were probed with mouse anti-human α-tubulin diluted 1 : 2000 ml (Sigma) and stained with a rabbit anti-mouse secondary antibody coupled with horseradish peroxidase, diluted 1 : 5000 ml (Sigma). Bands were visualized using an enhanced chemiluminescence protocol (Pierce) and radiographic film (Kodak). For cyclin B1 immunoblots, cells were seeded in 12-well plates at 1×10^5 cells per well in complete medium and treated with different concentrations of **15a**, **15b** and **15e** for 24 h. After treatment, cells were washed twice with phosphate-buffered saline and lysed in 1× SDS sample buffer. Proteins were separated, transferred, probed and analyzed similar to tubulin. The primary anti-cyclin B1 antibody was employed at 1 : 1500 (Sigma) and horseradish peroxidase coupled goat anti-rabbit secondary antibody diluted 1 : 5000 (Sigma).[24]

RT-PCR analysis. Total RNA was isolated using the TRIzol reagent (Invitrogen). Semiquantitative RT-PCR was carried out essentially as described previously.[27] RNA was reverse transcribed using reagents from the first-strand cDNA synthesis

kit (Fermentas). Primers p21F (5′-GCACCCTAGTTCTACCTCAG-GCAGCTC-3′) and p21R (5′-GACACAGAACAGTACAGGGTGTG-GTCC-3′) were used for the amplification of human p21 mRNA. Primers GAPDHF (5′-GCCAACGTGTCAGTGGT-GGACCTG-3′) and GAPDHR (5′-CAGCAGTGAGGGTCTCTCT-CTTCC-3′) were used for the amplification of human GAPDH. The PCR conditions for p21 and GAPDH were: 1 cycle of 3 min at 95 °C; 37 cycles of 1 min at 95 °C, 1 min at 60 °C and 1 min at 72 °C; and 1 cycle of 7 min at 72 °C for 22 cycles.

Immunohistochemistry of tubulin and analysis of nuclear morphology. HeLa cells were seeded on a glass cover slip, incubated for 24 h in the presence or absence of test compounds **15a**, **15b** and **15e** at a concentration of 2 μM. Cells grown on coverslips were fixed in 3.5% formaldehyde in phosphate-buffered saline (PBS) pH 7.4 for 10 minutes at room temperature. Cells were permeabilized for 6 minutes in PBS containing 0.5% Triton X-100 (Sigma) and 0.05% Tween-20 (Sigma). The permeabilized cells were blocked with 2% BSA (Sigma) in PBS for 1 h. Later, the cells were incubated with the primary antibody for tubulin from Sigma at 1 : 200 diluted in blocking solution for 4 h at room temperature. Subsequently the antibodies were removed and the cells were washed thrice with PBS. Cells were then incubated with the FITC labeled anti-mouse secondary antibody (1 : 500) for 1 h at room temperature. Cells were washed thrice with PBS and mounted in medium containing DAPI. Images were captured using an Olympus confocal microscope and analyzed with Provision software.

Molecular modelling. AutoDock was used to dock 3,4,5-trimethoxybiphenyl derivatives in the colchicine binding site of tubulin.[35,36] Initial Cartesian coordinates for the protein–ligand complex structure were derived from the crystal structure of tubulin (PDB ID: 3E22). The protein targets were prepared for molecular docking simulation by removing water molecules and bound ligands. Hydrogen atoms and Kollman charges were added to each protein atom. Auto-Dock Tools (ADT) were used to prepare and analyze the docking simulations for the AutoDock program. Coordinates of each compound were generated using Chemdraw11 followed by MM2 energy minimization. A grid map in Autodock that defines the interaction of protein and ligands in the binding pocket was defined. The grid map was used with 60 points equally in x, y, and z directions. AutoGrid 4 was used to produce grid maps for AutoDock calculations where the search space size utilized grid points of 0.375 Å. The Lamarckian genetic algorithm was chosen to search for the best conformers. Each docking experiment was performed 100 times, yielding 100 docked conformations. Parameters used for the docking were as follows: a population size of 150; a random starting position and conformation; a maximal mutation of 2 Å in translation and 50 degrees in rotations; an elitism of 1; a mutation rate of 0.02 and a crossover rate of 0.8; and a local search rate of 0.06. Simulations were performed with a maximum of 1.5 million energy evaluations and a maximum of 50 000 generations. Final docked conformations were clustered using a tolerance of 1.0 Å root mean square deviation. The best model was picked based on the best stabilization energy. The final figures for molecular modeling were generated by using PyMol.[37]

Acknowledgements

Notes and references

1 M. A. Jordan and L. Wilson, *Nat. Rev. Cancer*, 2004, **4**, 253–265.
2 C. Dumontet and M. A. Jordan, *Nat. Rev. Drug Discovery*, 2010, **9**, 790–803.
3 E. A. Perez, *Mol. Cancer Ther.*, 2009, **8**, 2086–2095.
4 M. A. Jordan and K. Kamath, *Curr. Cancer Drug Targets*, 2007, **7**, 730–742.
5 F. Pellegrini and D. R. Budman, *Cancer Invest.*, 2005, **23**, 264–273.
6 G. C. Tron, T. Piral, G. Sorba, F. Pagliai, S. Busacca and A. A. J. Genazzani, *Med. Chem.*, 2006, **49**, 3033–3044.
7 A. Chaudhary, S. N. Pandeya, P. Kumar, P. P. Sharma, S. Gupta, N. Soni, K. K. Verma and G. Bhardwaj, *Mini-Rev. Med. Chem.*, 2007, **7**, 1186–1205.
8 S. Arora, X. I. Wang, S. M. Keenan, C. Andaya, Q. Zhang, Y. Peng and W. J. Welsh, *Cancer Res.*, 2009, **69**, 1910–1915.
9 F. Medrano, J. M. Andreu, M. J. Gorbunoff and S. N. Timasheff, *Biochemistry*, 1989, **28**, 5589–5599.
10 B. L. Flynn, E. Hamel and M. K. Jung, *J. Med. Chem.*, 2002, **45**, 2670–2673.
11 S. Y. Sharp, K. Boxall, M. Rowlands, C. Prodromou, S. M. Roe, A. Maloney, M. Powers, P. A. Clarke, G. Box, S. Sanderson, L. Patterson, T. P. Matthews, K. M. Cheung, K. Ball, A. Hayes, F. Raynaud, R. Marais, L. Pearl, S. Eccles, W. Aherne, E. McDonald and P. Workman, *Cancer Res.*, 2007, **67**, 2206–2216.
12 M. S. Squires, R. E. Feltell, N. G. Wallis, E. J. Lewis, D. M. Smith, D. M. Cross, J. F. Lyons and N. T. Thompson, *Mol. Cancer Ther.*, 2009, **2**, 324–332.
13 L. Santo, S. Vallet, T. Hideshima, D. Cirstea, H. Ikeda, S. Pozzi, K. Patel, Y. Okawa, G. Gorgun, G. Perrone, E. Calabrese, M. Yule, M. Squires, M. Ladetto, M. Boccadoro, P. G. Richardson, N. C. Munshi, K. C. Anderson and N. Raje, *Oncogene*, 2010, **29**, 2325–2336.
14 X. Li, X. Lu, M. Xing, X. H. Yang, T. T. Zhao, H. B. Gong and H. L. Zhu, *Bioorg. Med. Chem. Lett.*, 2012, **22**, 3589–3593.
15 A. Kamal, A. B. Shaik, N. Jain, C. Kishor, A. Nagabhushana, B. Supriya, G. BharathKumar, S. S. Chourasiya, Y. Suresh,

R. K. Mishra and A. Addlagatta, *Eur. J. Med. Chem.*, 2015, **92**, 501–513.

16 R. LeBlanc, J. Dickson, T. Brown, M. Stewart, H. N. Pati, D. VanDerveer, H. Arman, J. Harris, W. Pennington, Jr., H. HL and M. Lee, *Bioorg. Med. Chem.*, 2005, **13**, 6025–6034.

17 R. Zaninetti, S. V. Cortese, S. Aprile, A. Massarotti, P. L. Canonico, G. Sorba, G. Grosa, A. A. Genazzani and T. Pirali, *ChemMedChem*, 2013, **4**, 633–643.

18 (*a*) B. J. Leslie, C. R. Holaday, T. Nguyen and P. J. Hergenrother, *J. Med. Chem.*, 2010, **53**, 3964–3972; (*b*) S. F. Wang, Y. Yin, Y. L. Zhang, S. W. Mi, M. Y. Zhao, P. C. Lv, B. Z. Wang and H. L. Zhu, *Eur. J. Med. Chem.*, 2015, **93**, 291–299.

19 X. H. Yang, Q. Wen, T. T. Zhao, J. Sun, X. Li, M. Xing, X. Lu and H. L. Zhu, *Bioorg. Med. Chem.*, 2012, **20**, 1181–1187.

20 Y. Yin, F. Qiao, L. Y. Jiang, S. F. Wang, S. Sha, X. Wu, P. C. Lv and H. L. Zhu, *Bioorg. Med. Chem.*, 2014, **22**, 4285–4292.

21 B. Abu Thaher, M. Arnsmann, F. Totzke, J. E. Ehlert, M. H. Kubbutat, C. Schächtele, M. O. Zimmermann, P. Koch, F. M. Boeckler and S. A. Laufer, *J. Med. Chem.*, 2012, **55**, 961–965.

22 Su. Rehman, Mu. Rahman, V. K. Tripathi, J. Singh, T. Ara, S. Koul, S. Farooq and A. Kaul, *Bioorg. Med. Chem. Lett.*, 2014, **24**, 4243–4292.

23 S. F. Wang, Y. Yin, Y. L. Zhang, S. W. Mi, M. Y. Zhao, P. C. Lv, B. Z. Wang and H. L. Zhu, *Eur. J. Med. Chem.*, 2015, **26**, 291–299.

24 A. Kamal, A. B. Shaik, S. Polepalli, G. B. Kumar, V. S. Reddy, R. Mahesh, S. Garimella and N. Jain, *Bioorg. Med. Chem.*, 2015, **23**, 1082–1095.

25 A. Kamal, V. S. Reddy, A. B. Shaik, G. B. Kumar, M. V. Vishnuvardhan, S. Polepalli and N. Jain, *Org. Biomol. Chem.*, 2015, **13**, 3416–3431.

26 A. Kamal, A. B. Shaik, S. Polepalli, V. S. Reddy, G. B. Kumar, S. Gupta, K. V. Krishna, A. Nagabhushana, R. K. Mishra and N. Jain, *Org. Biomol. Chem.*, 2014, **12**, 7993–8007.

27 R. Zhou, C. Wang, H. Song and Z. He, *Org. Lett.*, 2010, **12**, 976–979.

28 G. C. Tron, T. Pirali, G. Sorba, F. Pagliai, S. Busacca and A. A. Genazzani, *J. Med. Chem.*, 2006, **49**, 3033–3044.

29 D. Kumar, N. M. Kumar, M. P. Tantak, M. Ogura, E. Kusaka and T. Ito, *Bioorg. Med. Chem. Lett.*, 2014, **24**, 5170–5174.

30 A. L. Wolfe, K. K. Duncan, N. K. Parelkar, S. J. Weir, G. A. Vielhauer and D. L. Boger, *J. Med. Chem.*, 2012, **55**, 5878–5886.

31 X. H. Yang, Q. Wen, T. T. Zhao, J. Sun, X. Li, M. Xing, X. Lu and H. L. Zhu, *Bioorg. Med. Chem.*, 2012, **20**, 1181–1187.

32 C. E. Walczak and R. Heald, *Int. Rev. Cytol.*, 2008, **265**, 111–158.

33 G. M. Morris, D. S. Goodsell, R. S. Halliday, R. Huey, W. E. Hart, R. K. Belew and A. J. Olson, *J. Comput. Chem.*, 1998, **19**, 1639–1662.

34 Y. Lu, J. Chen, M. Xiao, W. Li and D. D. Miller, *Pharm. Res.*, 2012, **29**, 2943–2971.

35 R. B. Ravelli, B. Gigant, P. A. Curmi, I. Jourdain, S. Lachkar, A. Sobel and M. Knossow, *Nature*, 2004, **428**, 198–202.

36 *AutoDock, version 4.0*; http://www.scripps.edu/mb/olson/doc/autodock/.

37 W. L. DeLano, DeLano Scientific, San Carlos, CA, USA, http://www.pymol.org, 2002.